Kinetic Isotope Effects for Nonadiabatic Proton Transfer Reactions in a Polar Environment. 1. Interpretation of Tunneling Kinetic Isotopic Effects

Philip M. Kiefer[†] and James T. Hynes*[,†,‡]

Department of Chemistry and Biochemistry, University of Colorado, Boulder, Colorado 80309-0215, and Département de Chimie, CNRS UMR 8640 PASTEUR, Ecole Normale Supérieure, 24, rue Lhomond, 75231 Paris, France

Received: July 22, 2004; In Final Form: September 22, 2004

A theoretical study of primary kinetic isotope effects (KIEs) is presented for proton transfer (PT) reactions in a polar environment in the nonadiabatic, i.e., tunneling, regime. This treatment differs from traditional descriptions for PT most notably in the identification of a solvent coordinate as the reaction coordinate. The theory explicitly addresses KIE features that are extremely sensitive to the proton donor−proton acceptor mode dynamics. Besides KIE behaviors that are *not* consistent with *nontunneling* PT, individual KIE aspects in some cases, such as magnitude, temperature dependence, variation with reaction asymmetry, and Swain−Schaad behavior can yield results consistent with *nontunneling* PT. However, a combination of KIE aspects—with particular emphasis on KIE variation with reaction asymmetry or temperature—can clearly identify tunneling in PT systems. In addition, PT via excited proton vibrational states is shown to significantly contribute to the reaction rate and KIEs, especially for extremely asymmetric reactions, where it can dominate.

1. Introduction

Proton transfer (PT) is of obvious importance in chemistry and biology.[1] Of particular interest is the growing attention to the occurrence of tunneling in PT reactions,[2−4] signaled primarily by the observation of large primary kinetic isotope effects (KIEs). In these reactions, it is apparent that the proton donor−proton acceptor mode, often called a "promoting" or "gating" mode,[2−7] has a significant impact. When this PT occurs in a hydrogen-bonded (H-bonded) AH···B complex, e.g.

$$AH\cdots B \rightleftharpoons A^{-}\cdots HB^{+} \tag{1.1}$$

the relevant coordinate would be the H-bond coordinate, e.g. the A···B separation.[8] Such coupling between H-bond dynamics and tunneling rates has, for example, been implicated in a variety of enzymatic reactions,[2−4,6] and KIEs have been used to characterize the H-bond dynamics.[2−4,6] In addition to large KIEs $k_H/k_D > 10$, anomalous Swain−Schaad ratios and non-Arrhenius temperature dependencies are proposed to be signatures of a tunneling process.[2]

This paper extends previous work on nonadiabatic, i.e., tunneling, PT reactions by this group[5] to explicitly examine KIE trends, with emphasis on effects due to the H-bond mode dynamics and excited proton vibrational state transitions. The "nonadiabatic" terminology refers to the perspective that tunneling can be regarded as a (nuclear) nonadiabatic transition between diabatic proton vibrational levels localized in the reactant and product wells.[5,6] With this formalism, we analyze four KIE trends for tunneling PT reactions to assist in clarification and analysis of KIE behavior: (i) KIE magnitude, (ii) temperature dependence, (iii) variation with reaction asymmetry, and (iv) the Swain−Schaad relationship connecting ratios of isotope effects,[11] e.g., $k_H/k_T = (k_D/k_T)^{3.3}$.

This formalism uses a nontraditional view for PT in solution and other polar environments.[5,6,12] In this perspective, the reaction coordinate is rearrangement of the environment surrounding the H-bond complex and does not include proton motion: after a suitable rearrangement, proton tunneling then occurs, through an *electronically* adiabatic barrier. In the resulting rate constant, this rearrangement cost largely determines the activation free energy, while the tunneling features enter as a prefactor.[5] This contrasts with the "traditional" view[1,13,14] where the reaction coordinate explicitly includes classical proton motion. In the traditional view, a tunneling correction is added to the rate expression to account for the transmission probability through the reaction barrier.[13−16] The one-dimensional picture for this correction is often referred to as "Bell" tunneling,[16] while the multidimensional tunneling picture is denoted as "corner-cutting" .[15,17]

Further, the standard picture normally makes no reference to the solvent. To the degree that the solvent is included, it is imagined to alter the rate via a differential equilibrium solvation of the TS and the reactant.[1,13−17] However, the equilibrium solvation assumption—which requires that the solvent motion is fast compared to the relevant motion of the reacting solutes in the TS region—is not at all plausible in the case of high frequency quantum proton motion; indeed, the opposite situation is more appropriate: the solvent is generally slow compared to the proton motion.[5,6,12,18−20]

The outline of the remainder of the paper is the following. After a review of the general picture and formalism of nonadiabatic PT in section 2, section 3 presents the KIE behavior arising from this formalism. Concluding remarks are offered in section 4.

* To whom correspondence should be sent. Telephone: (303) 492−6926. FAX: (303) 492−5894. E-mail: hynes@spot.colorado.edu.
† University of Colorado.
‡ Ecole Normale Supérieure.

10.1021/jp040497p CCC: $27.50 © 2004 American Chemical Society
Published on Web 12/02/2004

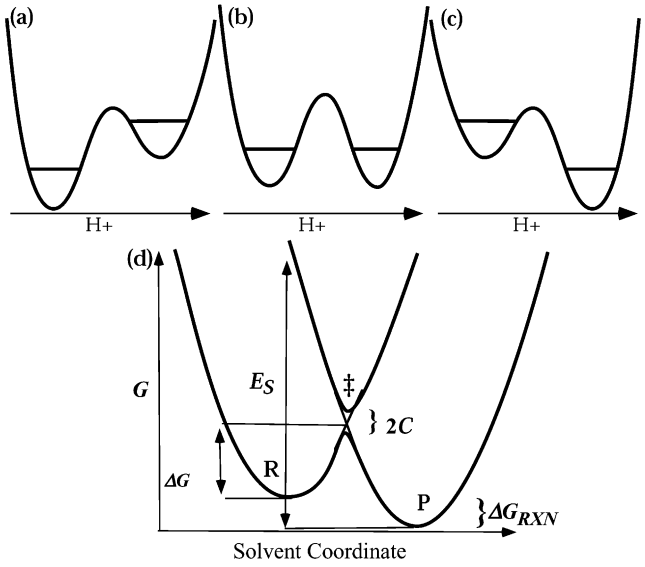

Figure 1. Free energy curves vs proton position at (a) the reactant R, (b) transition state ‡, and (c) product state P solvent configurations. In each case, the ground diabatic proton vibrational energy levels are indicated for both the reactant and product proton wells. (d) Free energy curves vs the solvent coordinate for both diabatic proton levels displayed in parts a−c.

2. Proton Nonadiabatic Tunneling Theory

Here we briefly review the key aspects of the tunneling rate constant formulation of ref 5. We begin with a review of the basic PT tunneling regime picture and the role of the H-bond mode, followed by the rate constant formulation including this mode, but restrict PT to involving only the ground proton vibrational state. The rate constant including excited proton vibrational levels is then discussed.

2a. General Perspective. 2a.1. Preliminary Fixed H-Bond Picture. In the underlying picture of PT reactions[5,7,12,18−20] employed within, the reaction is driven by configurational changes in the surrounding polar environment—a feature of much modern work on PT reactions,[5,7,12,18−21] and the reaction activation free energy is largely determined by the reorganization of this environment. The physical picture is displayed in Figure 1, with a fixed H-bond separation, a constraint later relaxed. The system free energy as a function of the proton coordinate—involving the electronically *adiabatic* proton potential—is displayed with the reactant and product *diabatic* proton vibrational states indicated, for three values of the solvent coordinate characterizing different environmental configurations: reactant state **R** (Figure 1a), transition state (TS) ‡ (Figure 1b), and product state **P** (Figure 1c). The **R** and **P** proton diabatic levels in Figure 1a−c are found by solving the nuclear Schrödinger equation for the proton in each of the reactant and product wells, respectively. (*Adiabatic* proton levels are found by solving the Schrödinger equation for the entire proton potential.) The evolving diabatic ground proton vibrational states define free energies as a function of the environment rearrangement, shown in Figure 1d. The reaction free energy barrier is due to the solvent, and at the TS solvent configuration, the proton potential is a symmetric double well, Figure 1b. At this thermally activated TS position, the proton reactant diabatic vibrational state is in resonance with the corresponding ground proton product state, and the proton can thus tunnel. This view is in stark contrast with the traditional picture for PT where the reaction coordinate and barrier are associated with the proton coordinate, and tunneling is a correction.[15−17]

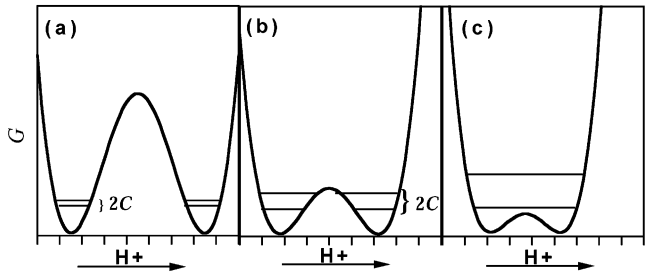

Figure 2. Variation of proton potentials at the reaction transition state configuration with decreasing AB separation, going from part a to part c. Both the ground and first excited proton *adiabatic* vibrational levels are indicated.

For the picture in Figure 1, the rate constant for nonadiabatic PT between reactant and product proton ground vibrational states with the H-bond separation (hereafter Q) fixed is[5,18,20]

$$k = \frac{C^2}{\hbar}\sqrt{\frac{\pi}{E_S RT}}\exp\left[-\frac{\Delta G^{\ddagger}}{RT}\right] \tag{2.1}$$

where the free energy barrier $\Delta G^{\ddagger}$ is

$$\Delta G^{\ddagger} = \frac{(\Delta G_{RXN} + E_S)^2}{4E_S} \tag{2.2}$$

and ΔG_{RXN} is the reaction asymmetry in Figure 1d, and E_S is the solvent reorganization (free) energy. The tunneling probability is governed by the square of the proton coupling C (described in more detail below), and thus the PT rate constant in eq 2.1 involves the combination of thermal activation to the TS in the solvent coordinate and the tunneling transmission probability at that TS.[22]

2a.2. H-Bond Mode and Proton Coupling. Figure 1 depicts what we term the proton nonadiabatic regime, in which the quantized diabatic proton vibrational levels lay below the barrier in the electronically adiabatic proton potential at the environment's TS configuration (Figure 1b). Figure 2 displays proton potentials and *adiabatic* proton vibrational levels for the environment's TS configuration for three different proton donor−proton acceptor (H-bond) distances, three different Q values.[25] Starting with large Q, Figure 2a has the proton ground and first excited *adiabatic* vibrational levels below the proton barrier. As Q is decreased, the proton barrier decreases. In Figure 2b, the proton levels still lie below the barrier. In both cases, the diabatic levels (e.g., Figure 1b) are split by twice the coupling C, which determines the tunneling probability between the diabatic levels. This coupling increases as the H-bond coordinate Q decreases, as the proton potential barrier for tunneling is lower and narrower. This is a key and strong dependence.

We pause to observe that for small enough Q, Figure 2c, the adiabatic levels lie above the proton barrier, and while the proton motion is still quantum, the reaction is no longer tunneling.[21] Figure 2 emphasizes that attention must be paid to whether the H-bond vibration remains at large values where PT is a nonadiabatic transition (tunneling, Figure 2, parts a and b), or whether the H-bond vibration allows the system to reach a small enough separation such that the proton vibration adiabatically follows the environment's slower rearrangement (nontunneling, Figure 2c).[26] Here we restrict ourselves to PT systems that are entirely nonadiabatic.[29] (KIEs for adiabatic nontunneling PT reactions have been presented elsewhere.[30]) Finally, we refer

to proton transfer throughout, but the theory applies to H atom and hydride transfer as well.[8]

As noted above, the splitting C increases as the H-bond separation decreases, e.g. going from Figure 2a to Figure 2b, due to the increased tunneling probability for a smaller proton barrier. The Q dependence of C is exponential, which can be understood via a semiclassical formula[5b,e,31]

$$C(Q) \approx \frac{\hbar\sqrt{\omega_R\omega_P}}{2\pi}\exp\left[-\frac{\pi}{\hbar\omega^{\ddagger}}(V^{\ddagger} - \mathrm{ZPE})\right] \qquad (2.3)$$

in which C depends on the TS proton potential properties: the curvatures in the wells, ω_R and ω_P, and at the top of the barrier $\omega^{\ddagger}$, as well as the barrier height $V^{\ddagger}$ in the proton coordinate. The difference $V^{\ddagger} - \mathrm{ZPE}$, where ZPE is the zero-point energy of the proton, $\mathrm{ZPE} \approx \hbar\omega_R/2$, is the vertical distance from the ground proton vibrational level to the top of that barrier. The frequencies in eq 2.3 contain the sole mass dependence, $\omega \propto 1/\sqrt{m}$. The Q dependence in eq 2.3 predominantly resides in the change in proton barrier height $V^{\ddagger}$ vs Q. Model calculations for OH···O systems[21,27] and quantum chemistry calculations of NH···N systems[32] show that the change in $V^{\ddagger}$ vs Q in the tunneling regime is predominantly linear.[33] This behavior then leads via eq 2.3 to a predominantly linear exponential form

$$C_L(Q) = C_{eqL}\exp[-\alpha_L(Q - Q_{eq})]; \quad C_{eqL} = C_L(Q_{eq}) \quad (2.4)$$

where Q_{eq} is the equilibrium H-bond separation in the reactant state and α_L is the exponent characterizing the exponential dependence (L = H, D, and T).

The mass dependence in eq 2.4 is contained within α_L and C_{eqL}. In particular, α_L is expected to be of the form $\alpha_L \propto \sqrt{m_L}$ because the exponent in eq 2.3 is inversely proportional to the barrier frequency $\omega^{\ddagger}$. Evaluation of C for proton potentials derived from quantum chemistry and model calculations[21,27,32−34] confirms this (e.g., $\alpha_D \approx \sqrt{2}\,\alpha_H$, and $\alpha_T \approx \sqrt{3}\,\alpha_H$), with typical values[5] $\alpha_H \sim 25-35$ Å^{-1}. We will exploit this mass correlation throughout in analyzing KIEs.[35]

In evaluating rate constant expressions given below, we will use a proton coupling derived from a proton TS potential with a significant barrier $V^{\ddagger} = 25$ kcal/mol, so that the PT system remains in the tunneling regime, and with well and barrier frequencies consistent with an O···O system, $\omega_R^H = 3200$ cm^{-1} and $\omega_H^{\ddagger} = 2700$ cm^{-1}. D and T isotope frequencies are appropriately mass-scaled, and from eq 2.3, $C_{eqH} = 3.57 \times 10^{-4}$ kcal/mol, $C_{eqD} = 3.74 \times 10^{-6}$ kcal/mol, and $C_{eqT} = 1.27 \times 10^{-7}$ kcal/mol. Finally, α_H is chosen to be 28 Å^{-1}, and $\alpha_D = 39.6$ Å^{-1} and $\alpha_T = 48.5$ Å^{-1} are appropriately mass-scaled.

2b. Proton Nonadiabatic "Tunneling" Formalism with Proton Donor—Acceptor Vibration. The importance of proton donor−proton acceptor modes in nonadiabatic PT has been emphasized in previous work.[5] We limit our discussion to a single mode—the H-bond mode—but other modes that regulate the barrier through which the proton must tunnel, e.g., H-bond bending modes,[6,30,36] can be dealt with in a similar manner. In this section, we summarize key aspects of the PT nonadiabatic formalism, referring the reader to ref 5 for a more detailed presentation, where a series of analytic forms for the rate constant were derived, each form corresponding to a specific regime. We first briefly present an extreme, purely quantum picture for the Q vibration in its ground vibrational state, and then proceed to higher temperatures T where the mode is progressively excited, ultimately becoming classical. For simplicity, we take a harmonic H-bond vibration $U_Q(Q) = U_{Q,eq} + (1/2)m_Q\omega_Q^2(Q - Q_{eq})^2$, with an effective mass m_Q and vibrational frequency ω_Q.[37] For the moment, we retain the restriction to PT between ground proton vibrational levels in the reactant and product.

For low temperatures $\hbar\omega_Q \gg RT$, the Q vibrational mode resides primarily in its ground state, and the PT rate expression is[5]

$$k_L = \frac{C_{00}^{\,2}}{\hbar}\sqrt{\frac{\pi}{E_S RT}}\exp\left[-\frac{(\Delta G_{RXN} + E_S)^2}{RT(4E_S)}\right] \qquad (2.5)$$

which is similar to eq 2.1 except that the proton coupling C is replaced by its quantum average over the ground Q-vibrational state

$$C_{00}^{\,2} = |\langle 0|C(Q)|0\rangle|^2 = C_{eqL}^{\,2}\exp\left[\alpha_L\Delta Q + \frac{(E_{\alpha L} - E_Q)}{\hbar\omega_Q}\right] \quad (2.6)$$

Here $\Delta Q = Q_{P,eq} - Q_{R,eq}$ is the difference in product and reactant equilibrium Q positions, and $E_Q = (1/2)m_Q\omega_Q^2\Delta Q^2$ is the associated reorganization energy. $E_{\alpha L}$ is a quantum energy term associated with the tunneling probability's variation with the Q vibration

$$E_{\alpha L} = \hbar^2\alpha_L^{\,2}/2m_Q \qquad (2.7)$$

Even with $\Delta Q = 0$ ($E_Q = 0$), C is increased from its fixed value $C(Q_{eq})$ by $\exp(E_{\alpha L}/\hbar\omega_Q)$: there is a finite probability of smaller H-bond separations even at low T due to zero point motion of Q. It is to be emphasized that this increase is larger for heavier particles for which $E_{\alpha L}$ is larger ($E_{\alpha L} \propto m_L$ since $\alpha_L \propto \sqrt{m_L}$). Here, the ratio $E_{\alpha L}/\hbar\omega_Q$ can be thought of as the square of the length scale of the C (tunneling probability) − H-bond mode coupling $\alpha_L^{\,2}$ times the average square quantum fluctuation of Q[5]

$$\alpha_L^{\,2}\langle(Q - Q_{eq})^2\rangle_{QM} = \alpha_L^{\,2}\frac{\hbar}{2m_Q\omega_Q} = \frac{E_{\alpha L}}{\hbar\omega_Q} \qquad (2.8)$$

The ratio $E_{\alpha L}/\hbar\omega_Q$ thus describes $E_{\alpha L}$ as a quantum energy scale for the localization of the Q wave function. If $E_{\alpha L}/\hbar\omega_Q \ll 1$, the coupling C is essentially that for fixed $Q = Q_{eq}$. As $E_{\alpha L}/\hbar\omega_Q$ increases, C increases, corresponding to increased quantum accessibility of smaller Q values.

For higher temperatures, the population of Q-vibrational excited states is increased, with the nth eigenstate with eigenenergy $E_n = \hbar\omega_Q(n + 1/2)$ probability given by $P_n = \exp(-\beta n\hbar\omega_Q)[1 - \exp(-\beta\hbar\omega_Q)]$. Now, there are a set of solvent free energy curves for both the reactant and product for each Q-vibrational state. Figure 3 displays this for the ground and first excited Q-vibrational state free energy curves for the reactant ($n = 0, 1$) and product ($m = 0, 1$), with each set of levels separated by one quantum of energy $\hbar\omega_Q$. PT thus can occur via a number of possible paths, starting from a thermal population of reactant Q-vibrational states. The arrows in Figure 3 correspond to two such paths: starting from either the ground or excited Q-vibrational state in the reactant and ending in the product ground Q-vibrational state. (For the system in Figure 3, there are two additional paths ending in the excited Q product

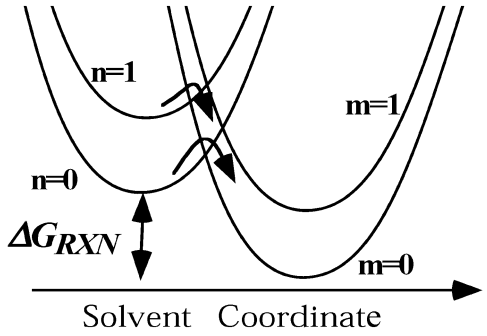

Figure 3. Proton diabatic free energy curves vs the solvent coordinate for individual reactant (n) and product (m) H-bond vibrational states.

vibrational state.) Each path has a reaction activation free energy barrier $\Delta G^{\ddagger}_{n\rightarrow m}$

$$\Delta G^{\ddagger}_{n\rightarrow m} = \frac{(\Delta G_{\mathrm{RXN}} + \Delta E_{nm} + E_{\mathrm{S}})^2}{4E_{\mathrm{S}}} \qquad (2.9)$$

where $\Delta E_{nm} = \hbar\omega_Q(m - n)$, and the transition probability at each TS (crossing point) involves the matrix element for C for the nth reactant and mth product Q vibrational states: $C_{nm} = \langle n|C(Q)|m\rangle$. For this dynamical Q perspective, the PT rate is the sum of all possible state-to-state transition contributions starting with a thermal distribution of reactant states[5a]

$$k_{\mathrm{L}} = \sum_n \sum_m P_n \frac{C_{nm}{}^2}{\hbar}\sqrt{\frac{\pi}{E_{\mathrm{S}}RT}}\exp\left[-\frac{\Delta G^{\ddagger}_{n\rightarrow m}}{RT}\right] \qquad (2.10)$$

For harmonic Q, C_{nm} is expressible in terms of Laguerre polynomials L[5a]

$$C_{nm}{}^2 = |\langle n|C(Q)|m\rangle|^2 =$$
$$C_{\mathrm{eq}}{}^2 e^{-\alpha_{\mathrm{L}}\Delta Q} e^{(E_{\alpha L}-E_Q)/\hbar\omega_Q}\left(\sqrt{\frac{E_{\alpha\mathrm{L}}}{\hbar\omega_Q}} - \sqrt{\frac{E_Q}{\hbar\omega_Q}}\right)^{2(n-m)} \times \frac{m!}{n!}\left[L_m^{n-m}\left(\frac{E_Q - E_{\alpha\mathrm{L}}}{\hbar\omega_Q}\right)\right]^2; \quad m \le n$$
$$= C_{\mathrm{eq}}{}^2 e^{-\alpha_{\mathrm{L}}\Delta Q} e^{(E_{\alpha\mathrm{L}}-E_Q)/\hbar\omega_Q}\left(\sqrt{\frac{E_{\alpha\mathrm{L}}}{\hbar\omega_Q}} + \sqrt{\frac{E_Q}{\hbar\omega_Q}}\right)^{2(m-n)} \times \frac{n!}{m!}\left[L_n^{m-n}\left(\frac{E_Q - E_{\alpha\mathrm{L}}}{\hbar\omega_Q}\right)\right]^2; \quad n \le m \qquad (2.11)$$

We briefly discuss, for future use, the activation energy for each transition in eq 2.10. The combination of the excitation probability P_n of the nth reactant state and the free energy barrier for each transition $\Delta G^{\ddagger}_{n\rightarrow m}$ gives

$$P_n \exp\left[-\frac{\Delta G^{\ddagger}_{n\rightarrow m}}{RT}\right] \propto \exp\left[-\frac{(n\hbar\omega_Q + \Delta G^{\ddagger}_{n\rightarrow m})}{RT}\right]$$
$$= \exp\left\{-\frac{\Delta G^{\ddagger}_{\mathrm{o}\rightarrow\mathrm{o}}}{RT} - \{[\hbar\omega_Q(m-n)]^2 + 2\hbar\omega_Q(m-n)\Delta G_{\mathrm{RXN}} + 2\hbar\omega_Q(m+n)E_{\mathrm{S}}\}/4RTE_{\mathrm{S}}\right\} \qquad (2.12)$$

One should note that the second exponent in eq 2.12, i.e., $n\hbar\omega_Q + \Delta G^{\ddagger}_{n\rightarrow m} - \Delta G^{\ddagger}_{\mathrm{o}\rightarrow\mathrm{o}}$, is symmetric upon interchange of n and m, if ΔG_{RXN} is inverted as well, e.g., the second argument of the activation energy with $m > n$ for an endothermic reaction, $\Delta G_{\mathrm{RXN}} > 0$, will be *identical* to that for an exothermic reaction of equal magnitude reaction asymmetry, $\Delta G_{\mathrm{RXN}} < 0$, with m and n switched. The significance of this, when combined with a similar symmetry $C_{nm}{}^2 = C_{mn}{}^2$ in eq 2.11, is the following. The combination of the activation barrier in eq 2.12 and $C_{nm}{}^2$ describes the n and m dependence for each contribution in eq 2.10. The symmetry of the combination implies that the contribution of excited H-bond vibrational states will symmetrically increase with increasing reaction asymmetry (increasing $|\Delta G_{\mathrm{RXN}}|$). This behavior is central to the reaction asymmetry dependence of rate constants and KIEs, to be discussed in section 3a.

Equation 2.10 gives the nonadiabatic PT rate constant expression for any temperature. For low temperatures $\hbar\omega_Q \gg RT$, the Q mode predominantly resides in its ground vibrational state, and eq 2.10 reduces to eq 2.5. As T is increased, contributions from excited Q vibrational states become more significant. For the intermediate regime $\hbar\omega_Q \sim RT$, many paths must be considered in eq 2.10, and for high temperatures $\hbar\omega_Q \ll RT$, the Q mode is classical and a continuum of levels is involved.

In these latter regimes, $\hbar\omega_Q \sim RT$ and $\hbar\omega_Q \ll RT$, the PT rate expression eq 2.10 can be simplified for $\Delta Q = 0$ to[5]

$$k_{\mathrm{L}} = \frac{\langle C^2\rangle}{\hbar}\sqrt{\frac{\pi}{(E_{\mathrm{S}} + \tilde{E}_{\alpha\mathrm{L}})RT}}\exp\left[-\frac{\Delta G^{\ddagger}_{\mathrm{L}}}{RT}\right] \qquad (2.13)$$

where the reaction barrier is given by

$$\Delta G^{\ddagger}_{\mathrm{L}} = \frac{(\Delta G_{\mathrm{RXN}} + E_{\mathrm{S}} + E_{\alpha\mathrm{L}})^2}{4(E_{\mathrm{S}} + \tilde{E}_{\alpha\mathrm{L}})} \qquad (2.14)$$

$$\tilde{E}_{\alpha\mathrm{L}} = E_{\alpha\mathrm{L}}(^1/_2)\beta\hbar\omega_Q \coth((^1/_2)\beta\hbar\omega_Q) \qquad (2.15)$$

where $\tilde{E}_{\alpha\mathrm{L}}$ is an isotope-dependent parameter via $E_{\alpha\mathrm{L}}$ with $\beta = 1/RT$: the ratio $\tilde{E}_{\alpha\mathrm{L}}/E_{\alpha\mathrm{L}}$ is the thermal average of the oscillator potential energy to the thermal value $RT/2$. The square proton coupling factor in eq 2.13 is the thermal average over the Q vibrational states[5]

$$\langle C^2\rangle = C_{\mathrm{L}}{}^2(Q_{\mathrm{eq}})\exp\left(2\frac{E_{\alpha\mathrm{L}}}{\hbar\omega_Q}\coth((^1/_2)\beta\hbar\omega_Q)\right) \qquad (2.16)$$

As one expects, α_{L} (via $E_{\alpha\mathrm{L}}$, eq 2.7) contributes significantly to the average in eq 2.16. In particular, the sensitivity of the coupling of C to Q dynamics is displayed in the ratio $E_{\alpha\mathrm{L}}/\hbar\omega_Q$ so that $\langle C^2\rangle$ increases as this ratio increases (cf. eq 2.8). As an example, a system with $E_{\alpha\mathrm{H}} = 1$ kcal/mol, $\hbar\omega_Q = 200$ cm^{-1}, and $T = 300$ K, gives a value of 7.8 for the argument in the exponent in eq 2.16, resulting in an ~2500-fold rate enhancement from the fixed $Q = Q_{\mathrm{eq}}$ value. Heavier particles will benefit even more from thermal activation of Q motion because $E_{\alpha\mathrm{L}}/\hbar\omega_Q$ is larger ($E_{\alpha\mathrm{L}} \propto m_{\mathrm{L}}$); for the above example with D instead of H, the rate enhancement from the Q fixed is ~$(2500)^2$-fold. Thus, the exponential in eq 2.16 *decreases* the KIE from a fixed Q value by ~2500-fold. The actual KIE magnitude is reflected by the isotopic ratio of eq 2.16. Using the C_{eq} values given at the end of section 2a, $C_{\mathrm{eq,H}}{}^2/C_{\mathrm{eq,D}}{}^2 = 9100$, the isotopic ratio of eq 2.16 is this fixed Q value reduced by ~2500-fold $\langle C^2\rangle_{\mathrm{H}}/\langle C^2\rangle_{\mathrm{D}} = 3.6$. Physically, the reduction in KIE is due to the heavier particle "waiting" for a larger compression in the H-bond coordinate to compensate for a weaker tunneling probability.

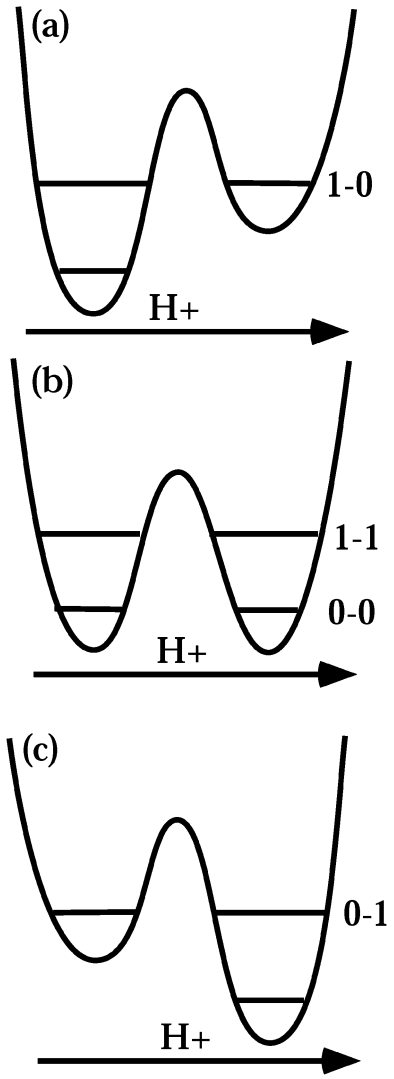

Figure 4. Proton potentials for the solvent coordinate TS for four proton vibrational transitions ($n_R - n_P$): (a) 1−0, (b) 0−0 and 1−1, and (c) 0−1. The lines indicate diabatic proton vibrational levels.

Also apparent in eq 2.16 is the increase of $\langle C^2 \rangle$ with temperature due to the increased probability of smaller Q separations, governed by the ratio $\hbar\omega_Q/RT$. Clearly, H-bond dynamics plays a critical role in the magnitude of rate constants and KIEs.

$E_{\alpha L}$ also appears in the reaction barrier in eq 2.14; $E_{\alpha L}$ appears as an energetic contribution to that barrier due to thermal activation of the H-bond mode. The isotopic dependence $E_{\alpha L} \propto m_L$ will play a key role in isotope and temperature effects, a theme discussed further within. First, however, we need to describe the inclusion of excited proton vibrational levels.[38]

2c. Excited Proton Product and Reactant Vibrational States. So far, PT has been assumed to occur from the reactant ground proton diabatic vibrational state to the corresponding state in the product. However, for very exothermic or endothermic reactions ($|\Delta G_{RXN}| \geq E_S + E_Q + \hbar\omega_L$), excited proton vibrational states will become important. The proton can be transferred into an excited proton product vibrational state for an exothermic case and from a thermally excited reactant proton vibration for an endothermic case. This is analogous to the Figure 3 H-bond mode picture, except that now each free energy curve will correspond to a diabatic proton vibrational level.

Figure 4 presents the TS proton potentials where four such transitions are involved. Each TS or intersection of the proton diabatic free energy curves corresponds to a specific resonance situation. Figure 4b is the symmetric proton potential for the ground state-to-ground state (0−0) transition and the corresponding first excited-state transition (1−1). Note that the 1−1 transition will have a higher transition probability (larger C) because the excited proton level is closer to the proton barrier top. The increase in tunneling probability for the 1−1 transition comes, however, at a cost of 1 quantum of proton vibration excitation, which is added to the activation energy (analogous to that in eq 2.12, see also Figure 3). Parts a and c of Figure 4 show the proton potentials with 1−0 and 0−1 transitions, respectively. Both will have a reduced tunneling probability compared with the 0−0 transition due to a smaller barrier to tunnel through.[39] Starting on the ground proton vibrational reactant free energy curve, thermal excitation of the reactant proton vibrational mode leads to the 1−0 transition, assisting endothermic reactions, while extra solvent activation passed the 0−0 transition to the 0−1 transition assists exothermic reactions. The interplay between cost of thermal excitation and gain from increased tunneling probability and their isotope dependence will play a significant role in KIEs. This will be described further in section 3 with examples.

Excited proton vibrational states are included in the PT rate as a sum over all state-to-state PT rates $k_{n_R \rightarrow n_P}$ from a proton reactant state n_R to a product state n_P

$$k_L = \sum_{n_R}\sum_{n_P} P_{n_R} k_{n_R \rightarrow n_P} \tag{2.17}$$

where each state-to-state rate is weighted by the reactant state thermal occupation P_{n_R} ($P_{n_R} = \exp(-\beta E_{n_R})/\sum_{n_R} \exp(-\beta E_{n_R})$, and $E_{n_R} = \hbar\omega_R(n_R + {}^1/_2)$). $k_{n_R \rightarrow n_P}$ is given by eq 2.10

$$k_{n_R \rightarrow n_P} = \sum_n \sum_m P_n \frac{C_{nm}{}^2(n_R \rightarrow n_P)}{\hbar} \sqrt{\frac{\pi}{E_S RT}} \exp\left[-\frac{\Delta G^{\ddagger}_{n,m;n_R \rightarrow n_P}}{RT}\right] \tag{2.18}$$

except that the reaction free energy barrier $\Delta G^{\ddagger}_{n,m;n_R \rightarrow n_P}$ and coupling $C_{nm}(n_R \rightarrow n_P)$ are now transition-specific. The reaction asymmetry for each transition depends on the reactant and product states, and thus it alters the reaction barrier[5e]

$$\Delta G^{\ddagger}_{n,m;n_R \rightarrow n_P} = \frac{(\Delta G_{RXN} + \Delta E_{nm} + n_P\hbar\omega_P - n_R\hbar\omega_R + E_S)^2}{4E_S} \tag{2.19}$$

where ω_R and ω_P are the proton frequencies in the reactant and product states.

The proton coupling squared $C_{nm}{}^2(n_R \rightarrow n_P)$ is identical to that in eq 2.11

$$C_{nm}{}^2(n_R \rightarrow n_R) = |\langle n|C_{n_R,n_R}(Q)|m\rangle|^2 \tag{2.20}$$

except that $C_{eqL}(n_R \rightarrow n_P)$ is transition-dependent. $C_{eqL}(n_R \rightarrow n_P)$ increases as the quantum numbers n_R and n_P increase because the width and height of the proton coordinate barrier is smaller as the proton level sits higher in either well. Using proton potential parameters presented at the end of section 2a results in a significantly higher proton coupling, a ∼10-fold increase going from the 0−0 ($n_R = 0$ to $n_P = 0$) transition to either the 0−1 or 1−0 transition.[40] A good approximation for C_{eqL} for all the transitions involved is a variant of eq 2.3[40]

$$C_{\mathrm{eqL}}(n_{\mathrm{R}} \rightarrow n_{\mathrm{P}}) \approx \frac{\hbar\sqrt{\omega_{\mathrm{R}}\omega_{\mathrm{P}}}}{2\pi} \times \exp\left\{-\frac{\pi}{\hbar\omega^{\ddagger}}(V^{\ddagger} - (^1/_2)[(n_{\mathrm{R}}+1)\hbar\omega_{\mathrm{R}} + n_{\mathrm{P}}\hbar\omega_{\mathrm{P}}])\right\} \quad (2.21)$$

Hence, the proton coupling Q dependence $C_{n_{\mathrm{R}},n_{\mathrm{P}}}(Q)$ in eq 2.20 is written

$$C_{n_{\mathrm{R}},n_{\mathrm{P}}}(Q) = C_{\mathrm{eqL}}(n_{\mathrm{R}} \rightarrow n_{\mathrm{P}}) \exp[-\alpha_{\mathrm{L}}(Q - Q_{\mathrm{eq}})] \quad (2.22)$$

In principle, α_{L} in eq 2.22 is also transition-dependent, but calculations indicate that the dependence is not significant,[41] and we thus regard α_{L} as being isotope-dependent, but not transition-dependent. For example, the thermal average of C^2 for the moderate to high-temperature regime in eq 2.16 is accordingly

$$\langle C_{n_{\mathrm{R}},n_{\mathrm{P}}}{}^2\rangle = C_{\mathrm{eqL}}{}^2(n_{\mathrm{R}} \rightarrow n_{\mathrm{P}}) \exp\left(2\frac{E_{\alpha\mathrm{L}}}{\hbar\omega_Q}\coth((^1/_2)\beta\hbar\omega_Q)\right) \quad (2.23)$$

Equations 2.17 and 2.18 formally give the general nonadiabatic PT rate constant for all regimes. For low temperatures, the nonadiabatic PT rate only involves a few excitations in either the proton or H-bond mode. For moderate to high temperatures, more excitations are probable, and here the nonadiabatic PT rate is given by eq 2.17 with a modified version of eq 2.13 for $k_{n_{\mathrm{R}}\rightarrow n_{\mathrm{P}}}$

$$k_{n_{\mathrm{R}}\rightarrow n_{\mathrm{P}}} = \frac{\langle C_{n_{\mathrm{R}},n_{\mathrm{P}}}{}^2\rangle}{\hbar}\sqrt{\frac{\pi}{(E_{\mathrm{S}} + \tilde{E}_{\alpha\mathrm{L}})RT}}\exp\left[-\frac{\Delta G^{\ddagger}_{n_{\mathrm{R}},n_{\mathrm{P}}}}{RT}\right] \quad (2.24)$$

where the reaction barrier is altered from the 0−0 value in eq 2.14

$$\Delta G^{\ddagger}_{n_{\mathrm{R}},n_{\mathrm{P}}} = \frac{(\Delta G_{\mathrm{RXN}} + n_{\mathrm{P}}\hbar\omega_{\mathrm{P}} - n_{\mathrm{R}}\hbar\omega_{\mathrm{R}} + E_{\mathrm{S}} + E_{\alpha\mathrm{L}})^2}{4(E_{\mathrm{S}} + \tilde{E}_{\alpha\mathrm{L}})} \quad (2.25)$$

The above PT rate constant expressions will now be used to analyze KIE trends.

3. Nonadiabatic Proton Transfer Kinetic Isotope Effects

In this section, we present the KIE behaviors that follow from the nonadiabatic PT formalism of Sec. 2, focusing on the four KIE observables (i−iv) listed in the Introduction. We first discuss the KIE magnitude and its variation with reaction asymmetry, which serves to demonstrate the importance of excited proton and H-bond vibrational states, and then we examine the temperature dependence. The Swain−Schaad behavior concludes the KIE behavior discussion.

3a. Kinetic Isotope Effect Magnitude and Variation with Reaction Asymmetry. Traditional treatments of KIEs, including those invoking tunneling along a minimum energy path, predict that the KIE is maximal for a symmetric reaction $\Delta G_{\mathrm{RXN}} = 0$.[42] We now present the nonadiabatic PT KIE vs reaction asymmetry behavior, and show that a similar behavior results. During the course of our discussion, the magnitude of tunneling PT KIEs will also be presented.

3a.1. Low Temperatures and High H-Bond Frequencies. The reaction free dependence for the extreme low-temperature regime $\hbar\omega_Q \gg RT$ eq 2.5 is isotope-independent (see note in section 2 about E_{S} isotope independence), and as such, no variation in KIE with reaction asymmetry is expected. To demonstrate the sensitivity to $\hbar\omega_Q/RT$ and the importance of excited proton and H-bond vibrational states even in this limit, we consider a system with $\hbar\omega_Q/RT$ larger than 1: $T = 200$ K; $\hbar\omega_Q = 500$ cm^{-1}, $\hbar\omega_Q/RT \sim 3.6$. We also use the parameters given at the end of section 2a.2, except that $V^{\ddagger} = 20$ kcal/mol, with $E_{\mathrm{S}} = 6$ kcal/mol, $\Delta Q = 0$, and $m_Q = 20$ amu.

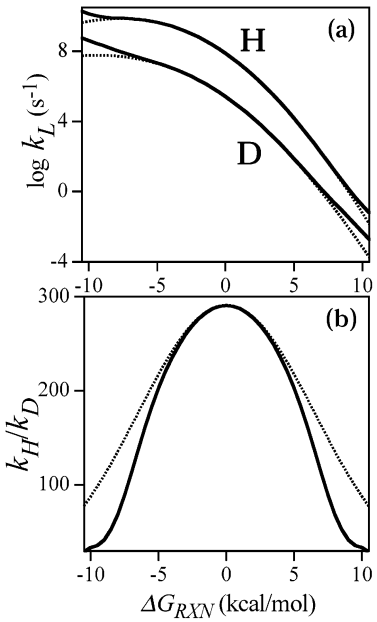

Figure 5. (a) Log rate constant vs reaction asymmetry for H and D (bold lines) using eqs 2.17 and 2.18 ($T = 300$ K; $\hbar\omega_Q = 1500$ cm^{-1}, $V^{\ddagger} = 20$ kcal/mol, $E_{\mathrm{S}} = 8$ kcal/mol, $\Delta Q = 0$, $m_{\mathrm{Q}} = 20$ amu, $\hbar\omega_{\mathrm{H}} = 3200$ cm^{-1}, $\hbar\omega_{\mathrm{H}}{}^{\ddagger} = 2700$ cm^{-1}, and $\alpha_{\mathrm{H}} = 28$ Å^{-1}. D parameters are appropriately mass scaled). Dotted lines indicate the logarithm of the rate constant exclusively for the 0−0 transition for both H and D. (b) KIE for the rates given in part a. Bold lines reflect the total rate constants and KIEs, while dotted lines reflect only those including the 0−0 transition.

The rates for PT and DT using eq 2.17 with eq 2.18 are plotted vs ΔG_{RXN} in Figure 5a. Also shown are the rates excluding any excitation by H or D in the reactant or product, i.e., only including the 0−0 proton transition. Excited proton states are clearly significant for more asymmetric cases ($|\Delta G_{\mathrm{RXN}}| > \hbar\omega_{\mathrm{L}}$) where the total rate differs from the 0−0 rate. Since $\hbar\omega_{\mathrm{H}} \sim 9$ kcal/mol $> \hbar\omega_{\mathrm{D}} \sim 6.4$ kcal/mol, the asymmetry at which the rate is not dominated by the 0−0 transition is smaller for D than for H.

We now turn to the KIEs of Figure 5a, displayed in Figure 5b. Both KIE trends are maximal for $\Delta G_{\mathrm{RXN}} = 0$ and drop off with increasing asymmetry. First note that the magnitude of the KIEs in Figure 5b is large (∼2 orders of magnitude), which is consistent with PT reactions in a fairly rigid H-bond complex, where tunneling is expected. Since no proton excitation is included in the 0−0 KIE, the KIE falloff here is due solely to differential isotopic excitation in the H-bond mode. Such a H-bond mode excitation gives an ∼3-fold decrease in KIE over the given reaction asymmetry range. Excitation in Q is more beneficial to the heavier D because C (which governs the tunneling probability) is more sensitive to Q for larger m_{L}, i.e., $E_{\alpha\mathrm{D}} > E_{\alpha\mathrm{H}}$ (see eq 2.11), and thus this falloff in KIE with increasing reaction asymmetry is due to a preferential increase in rate for D compared with H (see discussion of eq 2.12).

The next point of interest in Figure 5b is the significant impact on the KIE (another ∼2-fold decrease) from the contribution of H and D excitation for asymmetric reactions, visible from the KIE difference between the total rate and that for the 0−0

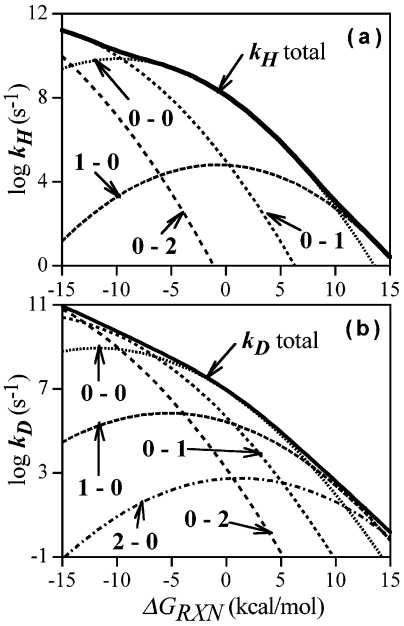

Figure 6. Log k vs reaction asymmetry ($T = 300$ K) for H (a) and D (b) including excited proton/deuteron vibrational states (solid lines). Broken lines indicate individual contributions from 0 to 0, 0−1, 1−0, 0−2, and 2−0 transitions. Rate constants were calculated with eqs 2.17 and 2.24 ($T = 300$ K; $\hbar\omega_Q = 300$ cm^{-1}, $V^{\ddagger} = 25$ kcal/mol, $E_S = 8$ kcal/mol, $m_Q = 20$ amu, $\hbar\omega_H = 3200$ cm^{-1}, $\hbar\omega_H^{\ddagger} = 2700$ cm^{-1}, and $\alpha_H = 28$ Å^{-1}. D parameters are appropriately mass scaled).

transition. Here the excited proton or deuteron vibrational states, with their increased coupling (tunneling probability), are more easily accessible for asymmetric reactions, and these excited levels are more thermally accessible for D than for H because $\hbar\omega_H > \hbar\omega_D$. Excitation in both the proton or deuteron and H-bond modes also becomes more significant for higher T, now discussed.

3a.2. Moderate and High Temperatures. To illustrate the KIE behavior for higher temperatures and softer H-bond complexes ($\hbar\omega_Q/RT \sim 1$ and $\hbar\omega_Q/RT < 1$), we consider a PT system with the parameters presented in section 2a, except that $T = 300$ K, $\hbar\omega_Q = 300$ cm^{-1}, $E_S = 8$ kcal/mol, and $V^{\ddagger} = 25$ kcal/mol. Here we use eq 2.17 with eq 2.24.

Parts a and b of Figure 6 display log k_L vs ΔG_{RXN} for H and D transfer, respectively, with the individual contributions of significant transitions $n_R \rightarrow n_P$ indicated. The increasing significance of the 0−1 and 0−2 transitions is apparent with increasing exothermicity, and that of the 1−0 and 2−0 transitions with increasing endothermicity. These transitions become significant for smaller reaction asymmetry for D than for H because $\hbar\omega_H > \hbar\omega_D$.[43]

The KIE for Figure 6 is displayed in Figure 7. The behavior is maximal at $\Delta G_{RXN} = 0$ and falls off with increasing reaction asymmetry, for the same reason discussed in section 3a.1. The KIE magnitude is, however, much smaller than that in Figure 5, due to the increased H-bond mode flexibility and the higher temperature. In fact, the KIE magnitude for fairly asymmetric reactions would be consistent with *nontunneling* PT. To emphasize this important point, the KIE with a slightly lower H-bond vibrational frequency $\hbar\omega_Q = 275$ cm^{-1} is also included in Figure 7. The KIE magnitude decreases by a factor of 3, emphasizing the sensitivity of the KIE to the donor−acceptor frequency. Again, this KIE behavior cannot be distinguished from that for nontunneling PT.

In summary, the maximal KIE behavior for tunneling PT is due to increased excitation in both the proton and H-bond

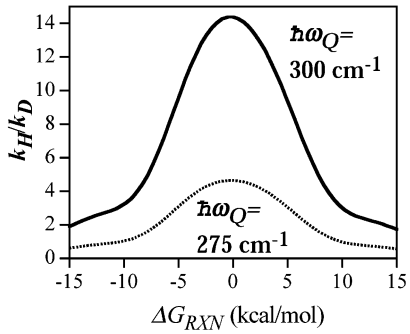

Figure 7. k_H/k_D for total rate constants in Figure 6 (solid line). The dotted line is the same PT system as the solid line, except that $\hbar\omega_Q = 275$ cm^{-1} rather than 300 cm^{-1}.

modes, excitations which become more facile with increased reaction asymmetry. Proton excitation increases the tunneling probability, via the proton coupling C eq 2.21, and because the deuteron mode is easier to excite than H, $\hbar\omega_H > \hbar\omega_D$, this benefits D more than H. Similarly, H-bond excitation also benefits D more than H because the D tunneling probability is more sensitive to changes in Q: see the $E_{\alpha L}/\hbar\omega_Q$ ratio in eqs 2.11 and 2.16 with $E_{\alpha H} < E_{\alpha D}$.

3a.3. Free Energy Relationship Analysis. The KIE variation with ΔG_{RXN} behavior just described for the moderate to high T regime will now be analyzed quantitatively. First, it will prove useful to present an isotope-dependent free energy relation for eq 2.17 with 2.24; the KIE vs ΔG_{RXN} behavior will then be deduced.

The PT rate's variation with reaction asymmetry, near $\Delta G_{RXN} = 0$, can be generally described by

$$\ln k_L = \ln k_L^o - \frac{\bar{\alpha}_{oL}\Delta G_{RXN}}{RT} - \frac{\bar{\alpha}'_{oL}\Delta G_{RXN}^2}{2RT} \qquad (3.1)$$

where k_L^o is the symmetric reaction $\Delta G_{RXN} = 0$ rate constant and $\bar{\alpha}_{oL}$ and $\bar{\alpha}'_{oL}$ are, respectively, the familiar Brønsted coefficient[1,14] and its derivative evaluated for the symmetric reaction

$$\bar{\alpha}_{oL} = -RT\left.\frac{\partial \ln k_L}{\partial \Delta G_{RXN}}\right|_o; \quad \bar{\alpha}'_{oL} = -RT\left.\frac{\partial^2 \ln k_L}{\partial \Delta G_{RXN}^2}\right|_o \qquad (3.2)$$

(The overbar notation is introduced to distinguish the Brønsted coefficient from the inverse coupling length α_L.) We begin the analysis by anticipating that the 0−0 rate k_{L00} will have a significant contribution near $\Delta G_{RXN} = 0$, and thus the rate expression in eq 2.17 can be written in terms of k_{L00} times the sum of the coefficients for each transition

$$k_L = k_{L00}\rho_L; \quad \rho_L = \sum_{n_R}\sum_{n_P} F_{n_R,n_P} \qquad (3.3)$$

where the transition coefficients are

$$F_{n_R,n_P} = P_{n_R}\exp\left[\frac{\pi(\hbar\omega_R n_R + \hbar\omega_P n_P)}{\hbar\omega^{\ddagger}}\right]\exp\left[-\frac{\Delta\Delta G^{\ddagger}_{n_R,n_P}}{RT}\right] \qquad (3.4)$$

Here $\Delta\Delta G^{\ddagger}_{n_R,n_P}$ is the difference between the general reaction barrier $\Delta G^{\ddagger}_{n_R,n_P}$ eq 2.25 and that, $\Delta G^{\ddagger}_{L0,0}$, for the 0−0 case

$$\Delta\Delta G^{\ddagger}_{n_R,n_P} = \Delta G^{\ddagger}_{n_R,n_P} - \Delta G^{\ddagger}_{L0,0} = [(n_P\hbar\omega_P - n_R\hbar\omega_R)(2(\Delta G_{RXN} + E_S + E_{\alpha L}) + n_P\hbar\omega_P - n_R\hbar\omega_R)]/4(E_S + \tilde{E}_{\alpha L}) \quad (3.5)$$

The second expression in eq 3.3 defines the sum as a rate constant enhancement factor ρ_L due to excited proton transitions from k_{L00}.

The parameters in eq 3.1 are derived in this perspective with the following results in Appendix A. The zero order contribution $\ln k^o_L$ to eq 3.1 involves the k_{L00} 0−0 rate evaluated for the symmetric reaction plus the rate enhancement ρ_{Lo} for $\Delta G_{RXN} = 0$ due to other transitions

$$\ln k^o_L = \ln k^o_{L00} + \ln \rho_{Lo} \quad (3.6)$$

For the $\hbar\omega_Q = 300$ cm^{-1} case in Figure 7, the rate is dominated by the 0−0 $\Delta G_{RXN} = 0$ rate, 99.8% for H and 88.9% for D. The dominance by the 0−0 rate is less with increasing mass because the excitation probability for heavier L is easier. The Brønsted coefficient $\bar{\alpha}_{oL}$ and its derivative $\bar{\alpha}'_{oL}$ in eq 3.1 are described by those for the 0−0 case plus a correction due to the contribution of excited proton vibrational transitions:

$$\bar{\alpha}_{oL} = (^1/_2)\frac{E_S + E_{\alpha L}}{(E_S + \tilde{E}_{\alpha L})} + \left\langle \frac{\partial\Delta\Delta G^{\ddagger}_{n_R,n_P}}{\partial\Delta G_{RXN}} \right\rangle_F \quad (3.7)$$

$$\bar{\alpha}'_{oL} = \frac{1}{2(E_S + \tilde{E}_{\alpha L})} - \left[\left\langle \left\langle \frac{\partial\Delta\Delta G^{\ddagger}_{n_R,n_P}}{\partial\Delta G_{RXN}} \right\rangle^2 \right\rangle_F - \left\langle \frac{\partial\Delta\Delta G^{\ddagger}_{n_R,n_P}}{\partial\Delta G_{RXN}} \right\rangle_F^2 \right] \quad (3.8)$$

The averages in eqs 3.7 and 3.8 are over the probability distribution $F_{n_R,n_P}|_o$ defined by eq 3.4 evaluated at $\Delta G_{RXN} = 0$ (see eq A.15).

For $\bar{\alpha}_{oL}$, the first term in eq 3.7—the 0−0 contribution—is slightly less than $^1/_2$ with a larger deviation for D because $E_{\alpha D} > E_{\alpha H}$. The excited-state contribution of the second term in eq 3.7 is small <0.1% for H and 1% for D, but because it is positive, it numerically cancels the deviation from $^1/_2$ in the first term, resulting in an isotope-independent $\bar{\alpha}_{oL} \approx {}^1/_2$.[45] In the context of TS structure, which is commonly associated with the Brønsted coefficient $\bar{\alpha}_L$,[1,13,14,21] the $\bar{\alpha}_{oL} = {}^1/_2$ value is here associated with the symmetric nature of the TS structure, i.e., the H (or D) diabatic levels in the reactant and product proton wells are degenerate. However, for asymmetry in the H-bond coordinate, e.g. $\Delta Q \neq 0$, one will have $\bar{\alpha}_{oL} \neq {}^1/_2$.[45]

For $\bar{\alpha}'_{oL}$, the 0−0 contribution in eq 3.8 (first term) is decreased by the excited proton state contribution (second term). This decrease is, however, small compared to the 0−0 $\bar{\alpha}'_{oL}$ contributions but is isotope-sensitive, <1% for H and 22% for D, so that the 0−0 contribution is dominant; that the second term in eq 3.8 is larger for D is due to the increased significance of its excited states compared with that for H. This has an impact for the isotope dependence of the FER, as discussed below.

The KIE behavior with reaction asymmetry is thus determined by the isotopic difference in FERs in eq 3.1, e.g. for H vs *D*

$$\ln(k_H/k_D) = \ln(k^o_H/k^o_D) - \frac{(\bar{\alpha}'_{oH} - \bar{\alpha}'_{oD})\Delta G_{RXN}^{\ 2}}{2RT} \quad (3.9)$$

where the position of the maximum in a KIE vs reaction asymmetry plot (H vs D) occurs for a symmetric reaction $\Delta G_{RXN} = 0$, a direct result of the isotope independence of eq 3.7.[45] The isotopic difference of eq 3.8 gives $\bar{\alpha}'_{oH} - \bar{\alpha}'_{oD} > 0$ because C is more sensitive to the H-bond mode dynamics for D than for H, $E_{\alpha D} > E_{\alpha H}$. The result is a decrease in KIE as the reaction asymmetry is increased for the reasons discussed above. The magnitude of the curvature in the KIE plot is determined by $\bar{\alpha}'_{oH} - \bar{\alpha}'_{oD}$, i.e., the isotopic difference of both terms in eq 3.8, and for the case in Figure 7, each term's isotopic difference contributes equally. The ~21% isotopic disparity between the size of the second term in eq 3.8 for H and D makes its isotopic difference significant.

3b. Temperature Behavior. The general temperature dependence of the PT rate eq 2.17 is certainly not Arrhenius, and thus it leads to nonlinear Arrhenius plots for both the rate and KIE (cf. ref 5e). However, within a limited temperature range, which is often the experimental situation, the rate and KIE can exhibit linear behavior in an Arrhenius plot, despite the tunneling character of the reaction. The T dependencies of rates and KIEs are now discussed for several regimes, and in the case of a limited temperature range, expressions for effective activation energies are obtained.

3b.1. Low Temperature. For *extremely* low T, $\hbar\omega_L$ and $\hbar\omega_Q \gg RT$, i.e., where there is only the 0−0 proton transition and no excitation in Q, the rate eq 2.5 applies and clearly appears to be Arrhenius, with an isotope-independent activation energy $E_{AL} = \Delta G^{\ddagger}$ eq 2.2.[46] The sole isotope dependence there arises from the tunneling prefactor C^2_{00}, the consequence of which is a T-independent KIE:

$$k_H/k_D = C_{00}^{H\ 2}/C_{00}^{D\ 2} \quad (3.10)$$

For negligible H-bond mode reorganization $\Delta Q \sim 0$ ($E_Q \sim 0$), eq 3.10 reduces to (cf. eq 2.6)

$$k_H/k_D = \exp\left[-\frac{E_{\alpha H}}{\hbar\omega_Q}\right] C_{oH}^{\ 2}(Q_{eq})/C_{oD}^{\ 2}(Q_{eq}) \quad (3.11)$$

where $E_{\alpha D} \sim 2E_{\alpha H}$ via mass scaling was used to simplify the exponential's argument. The KIE magnitude in this extreme quantum regime for Q still depends on $E_{\alpha H}$, despite no excitation in Q; this arises from the Q zero point motion (see discussion of eq 2.8). Consequently, even at very low T, H-bond mode motion decreases the KIE from its fixed Q value.

For slightly higher temperatures, excitations in both the H-bond mode and the proton vibration need to be included, as described in section 3a.1 (see Figure 5). To explore this, we consider the same system as in Figure 5, but vary T while keeping the reaction asymmetry fixed, $\Delta G_{RXN} = 0$. Figure 8a displays $\ln k_H$ and $\ln k_D$, using eq 2.17 with eq 2.18, vs $1/RT$ (T = 180−250 K). In this limited region, both H and D exhibit Arrhenius behavior, as expected from the lower temperature limit eq 2.5, except that the slopes are not identical (E_{AH} = 1.78 kcal/mol and E_{AD} = 2.29 kcal/mol), and they are slightly larger than that predicted by eq 2.5, where $E_{AH,D} = 1.5$ kcal/mol. The natural logarithm of the KIE T dependence from Figure 8a is displayed as Figure 8b. The actual behavior of this Arrhenius plot is nonlinear, but the solid line clearly indicates that the behavior could easily be mistaken for linear, within experimental error. The *apparent* activation energy for the KIE in Figure 8b is the difference in the slopes $E_{AD} - E_{AH} = 0.51$ kcal/mol in Figure 8a. The KIE temperature dependence is due to the differential H/D probability of H-bond and proton vibrational excitation with temperature. From Figure 8, we see for the first time that excitation of both the H-bond and proton vibrations will increase the activation energy from that solely due to the reaction free barrier $\Delta G^{\ddagger}$, i.e., that in eq 2.5. Furthermore, the increase in activation energy is larger for D

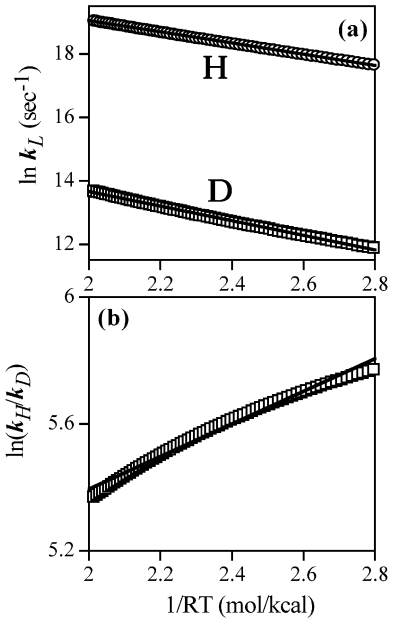

Figure 8. (a) ln k_H (○) and ln k_D (□) vs $1/RT$ ($T = 180-250$ K) for the PT system in Figure 5 with $\Delta G_{RXN} = 0$. (b) ln(k_H/k_D) (□) for rate constants in part a. Lines are linear fits to points. Slopes of lines give the activation energies: (a) $E_{AH} = 1.78$ kcal/mol and $E_{AD} = 2.29$ kcal/mol and (b) $E_{ADH} = 0.51$ kcal/mol.

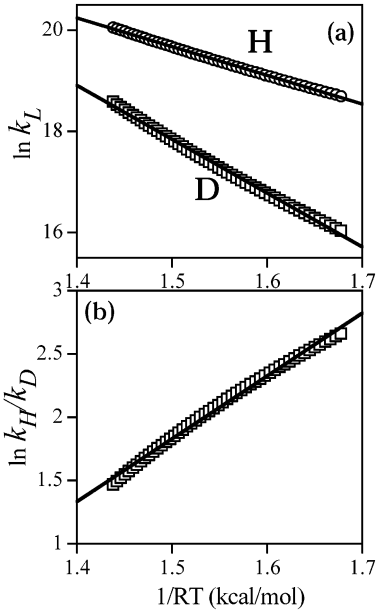

Figure 9. (a) ln k_H (○) and ln k_D (□) transfer rate constants vs $1/RT$ ($T = 300-350$ K) for the PT system in Figure 6 with $\Delta G_{RXN} = 0$. (b) k_H/k_D (□) for rate constants in part a. Lines are linear fits to points. Slopes of lines give the activation energies: (a) $E_{AH} = 5.66$ kcal/mol and $E_{AD} = 10.63$ kcal/mol and (b) $E_{ADH} = 4.97$ kcal/mol.

than for H, $E_{AD} > E_{AH}$. This is now discussed in more detail in the context of higher temperatures and lower H-bond frequencies, where quantitative analysis is more straightforward.

3b.2. Moderate to High Temperatures. For higher temperatures ($\hbar\omega_Q/RT \sim 1$ and $\hbar\omega_Q/RT < 1$), the T dependence of individual transition rates in eq 2.24 has two dominant contributions. The first is contained within the exponential containing the reaction free energy barrier, which gives Arrhenius behavior if the components of the reaction barrier, i.e., $\tilde{E}_{\alpha L}$ (see eq 2.15) and E_S,[47] have only a minor T dependence. The impact of such a T dependence is suppressed if the reorganization energy is significant ($E_S > E_{\alpha L}$). The second contribution to the T dependence comes from the thermally averaged square proton coupling eq 2.23, and in principle is not Arrhenius. In addition to these T dependencies for the individual transition rate constants, the thermal sum over excited proton transitions for the full rate in eq 2.17 is clearly also not Arrhenius. Altogether, these contributions give rise to a nonlinear T dependence in an Arrhenius plot, as expected for tunneling PT.[1,2,13,14,48] Nonetheless, we now show that this T dependence is effectively linear in an Arrhenius plot for a limited but nonnegligible temperature range. Even for data over a broad temperature range where nonlinear behavior is observed, our analysis should be useful to analyze different subregions in the nonlinear plot where the behavior is effectively linear. That is, we obtain rate and KIE expressions for a given T_o and the local slope in an Arrhenius plot at T_o.

In this analysis, the PT rate in proximity to a specific temperature T_o is written in an Arrhenius form

$$k_L = k_L(T_o)\exp[-(\beta - \beta_o)E_{AL}] \tag{3.12}$$

where the Arrhenius intercept is just the extrapolation from the rate at $T = T_o$ to infinite temperature: $A_L = k_L(T_o)\exp[\beta_o E_{AL}]$, and E_{AL} is determined by the slope in an Arrhenius plot.

For analysis purposes, we take the same system as described in section 3a.2, and vary the temperature ($T = 300-350$ K), while keeping the reaction asymmetry constant, $\Delta G_{RXN} = 0$. Figure 9 displays the apparent Arrhenius rate and KIE behavior in this limited T range. The apparent activation energies for H and D differ considerably, with E_{AD} almost twice E_{AH}: $E_{AH} = 5.66$ kcal/mol and $E_{AD} = 10.63$ kcal/mol; this results in a significant effective activation energy for the KIE $E_{AD} - E_{AH} = 4.97$ kcal/mol, displayed in Figure 9b. These slopes are now quantitatively analyzed to determine contributions from H-bond and proton vibration excitations.

We begin this analysis using the form for the rate expression given in eq 3.3 including excited proton vibrational states via the factor ρ_L, where the 0−0 rate k_{L00} is evaluated at the midrange temperature T_o, $k_{oL} = k_{L00}(T_o)$ (e.g., $T_o = 325$ K in Figure 9)

$$k_{oL} = \frac{C_{eqL}^{\,2}}{\hbar}\sqrt{\frac{\pi}{(E_S + \tilde{E}_{\alpha L})RT_o}} \times \exp\left(2\frac{E_{\alpha L}}{\hbar\omega_Q}\coth\left(\left({}^1/_2\right)\beta_o\hbar\omega_Q\right)\right)\exp\left[-\frac{\Delta G^{\ddagger}_{L0,0}}{RT_o}\right] \tag{3.13}$$

An Arrhenius form of eq 3.12 for the rate constant and its KIE is derived in Appendix B, where (cf. eqs B.12−B.15)

$$A_L = k_{oL}\rho_L(T_o)\exp(\beta_o E_{AL});$$
$$E_{AL} = E_{\alpha L}[\coth^2(\beta_o\hbar\omega_Q/2) - 1] + \Delta G^{\ddagger}_{L0,0} + \langle\Delta\Delta G^{\ddagger}_{n_R,n_P}\rangle_L \tag{3.14}$$

Here ρ_L is evaluated at T_o such that $k_L(T_o) = \rho_L k_{oL}$. $\Delta G^{\ddagger}_{L0,0}$ is the 0−0 reaction free energy barrier eq 2.25, and $\langle\Delta\Delta G^{\ddagger}_{n_R,n_P}\rangle_L$ is the activation free energy barrier contribution from excited proton states

$$\langle\Delta\Delta G^{\ddagger}_{n_R,n_P}\rangle_L = \frac{\sum_{n_R}\sum_{n_P} F_{oR,P}(\hbar\omega_R n_R + \Delta\Delta G^{\ddagger}_{n_R,n_P})}{\sum_{n_R}\sum_{n_P} F_{oR,P}} \tag{3.15}$$

where the symmetric reaction transition coefficient (cf. eq 3.4) is $F_{oR,P} = F_{n_R,n_P}(T = T_o)$. For the behavior in Figure 9, eq 3.14 gives reasonable estimates for E_{AH} and E_{AD}, $E_{AH} = 6.1$ kcal/mol and $E_{AD} = 11.2$ kcal/mol, which differ by less than 10% from the obtained numerical values. The decomposition of these apparent activation energies in eq 3.14 will prove to be useful in determining which contributions are more important and how these contributions change with T, $\hbar\omega_Q$, reaction asymmetry, and solvent reorganization energy E_S, as now discussed.

The first term in eq 3.14 is the activation energy contribution from the thermally averaged square coupling $\langle C^2 \rangle$ (see eq 2.23), and as such is extremely sensitive to parameters affecting the H-bond mode-tunneling coupling, namely T, $\hbar\omega_Q$, and $E_{\alpha L}$. For the present system, this term dominates the activation energy for both H (60%) and D (66%). Furthermore, since $E_{\alpha L} \propto m_L$ is mass sensitive, the predominant contribution to the activation energy difference determining the E_A for the KIE will be dominated by this first term. The coefficient $[\coth^2(\beta_o\hbar\omega_Q/2) - 1]$ in this term is extremely sensitive to T_o and $\hbar\omega_Q$, increasing drastically as T_o is increased or $\hbar\omega_Q$ decreases, and the ratio $\hbar\omega_Q/RT_o$ determines the relative contribution for this first term.

The second term in eq 3.14, the activation free energy barrier $\Delta G^{\ddagger}_{L0,0}$, is for the present system also significant for both H (39%) and D (25%). Of course, the magnitude of this term changes with reaction asymmetry, decreasing as the reaction goes from endo- to exothermic (cf. eq 2.19).

The last term in eq 3.14 for E_{AL} is the least important for the present system, <1% for H and 9% for D. Its lack of importance correlates with the significance of the 0−0 transition in the overall rate, described here by $\rho_L \sim 1$, $\rho_H = 1.004$ and $\rho_D = 1.25$. ρ_L will obviously change as the reaction becomes more asymmetric, as discussed in section 3a, as well as with increasing T.

With the above individual Arrhenius parameter results eq 3.14, we can now focus on those for the KIE, for the chosen system. The KIE Arrhenius slope is determined by the isotopic difference of E_{AL}s

$$E_{AD} - E_{AH} = E_{\alpha H}[\coth^2(\beta\hbar\omega_Q/2) - 1] + [\Delta G^{\ddagger}_{Do} - \Delta G^{\ddagger}_{Ho}] + [\langle \Delta\Delta G_{n_R,n_P}\rangle_D - \langle \Delta\Delta G_{n_R,n_P}\rangle_H] \quad (3.16)$$

The first term contributes the most, 72% as predicted above, the final difference is next in significance at 20%, and only 8% is observed for the middle difference. The minimal significance of the difference in 0−0 reaction barriers reflects the disparity $E_S > E_{\alpha L}$. The increased contribution of the excited proton state contribution is due to the differential contribution of the 0−0 transition to the total rate, $\rho_H < \rho_D$.

The Arrhenius intercept A_L in eq 3.14 is the extrapolation from the rate at $T = T_o$ $k_L(T_o) = k_{oL}\rho_L$ to infinite temperature, and thus the ratio of intercepts (H vs D) is the extrapolation of the KIE (H vs D) at T_o to infinite temperature

$$A_H/A_D = (k_H/k_D)_o \exp[-\beta_o(E_{AD} - E_{AH})] \quad (3.17)$$

where

$$(k_H/k_D)_o = (k_{oH}\rho_H/k_{oD}\rho_D) \quad (3.18)$$

The significant isotopic difference of Arrhenius intercepts, i.e., $A_H \neq A_D$, is a signature for a tunneling process[2]. For the system in Figure 9a, the Arrhenius prefactors have $A_H < A_D$, which is the case where eq 3.17 is less than 1. If, however, the system had $E_{AD} - E_{AH} \sim 1$ (not ~5 kcal/mol as in Figure 9), then one would have $A_H > A_D$, instead of $A_H < A_D$. Clearly, the interplay between the magnitude of $(k_H/k_D)_o$ and the difference $E_{AD} - E_{AH}$ determine whether $A_H > A_D$ or $A_H > A_D$. Thus, an alternate yet equivalent isotope analysis of Arrhenius plots would be to analyze $(k_H/k_D)_o$ and $E_{AD} - E_{AH}$ rather than A_H/A_D and $E_{AD} - E_{AH}$. The advantage of this alternative analysis is the direct connection between the KIE magnitude and Arrhenius slope with H-mode characteristics. Specifically, larger KIE magnitudes result from longer (large acid−base separations) and more rigid H-bond (large $\hbar\omega_Q/RT$) complexes, and small Arrhenius slopes arise with less probability of H-bond and proton mode excitation (i.e., low T and especially higher $\hbar\omega_Q/RT$ ratios), as can be seen from eq 3.14.

To expand on this and summarize the KIE temperature dependence, we note that Klinman et al.[2] have argued that the ratio A_H/A_D is an indication of the extent of tunneling at a specific temperature. In particular, these authors define three important regions a system goes through as the temperature is decreased: (I) starting at high T $A_H/A_D \sim 1$, (II) $A_H/A_D < 1$ for intermediate temperatures, and (III) $A_H/A_D > 1$ for low T. (Note that we have ignored the transition region between regimes II and III where $A_H/A_D \sim 1$.) In regime I, the proton is supposed not to tunnel, and the PT rate and KIE T behavior is Arrhenius. In both regimes II and III, the proton is supposed to tunnel, with more tunneling present in regime III.[2]

Within the present perspective, these three experimental possibilities indicate characteristics of the H-bond mode. Regime I occurs for smaller Q separations where the proton does not tunnel, but remains quantum, rather than classical, in character.[30] Regimes II and III refer to larger Q separations where the proton tunnels, while the distinction between regimes II and III lies primarily in the thermal population of the H-bond mode (i.e., primarily in $\hbar\omega_Q/RT$). As indicated above, a small $\hbar\omega_Q/RT$ value is likely to place a system in regime II, while a large $\hbar\omega_Q/RT$ value is likely to put a system in regime (II; i.e., regime III likely occurs for long and rigid H-bond complexes and low T, while regime II likely occurs for shorter and softer H-bond complexes at higher T. Of course, the possibility of a mixture of properties can give rise to either regime. For example, a short but rigid H-bond complex might be in either regime, depending on the magnitude of $(k_H/k_D)_o$ and the difference $E_{AD} - E_{AH}$, via eq 3.18. If $(k_H/k_D)_o$ is small, $E_{AD} - E_{AH}$ does not have to be as large if $(k_H/k_D)_o$ was larger, to get $A_H/A_D > 1$.

3c. Swain−Schaad Relationships. This final category of KIE behavior describes the relative KIEs between the three isotopes H, D, and T. For nontunneling PT perspectives, both the standard and nontraditional approaches,[13,14,30] the reactant and TS proton ZPEs associated with nontunneling KIEs give rise to specific relations between KIEs, Swain−Schaad relationships.[11,13,14] For purposes of discussion, we select the following Swain−Schaad relationship

$$\ln(k_H/k_T) = 3.3\ln(k_D/k_T) \quad (3.19)$$

Deviation from this relationship is regarded as a clear indication of tunneling.[2,7] Traditionally, the relationship has been experimentally assessed by varying system parameters and plotting $\ln(k_H/k_T)$ vs $\ln(k_D/k_T)$ and determining whether this produces a line which goes through the origin and has a slope ~ 3.3.[1b,11,13,14] However, eq 3.19 has also been assessed by plotting the ratio $\ln(k_H/k_T)/\ln(k_D/k_T)$ vs a system parameter, such as temperature.[2] If the ratio deviates significantly from 3.3, the PT system is said to be tunneling. In this section, we will examine whether a nonadiabatic tunneling PT system can exhibit the behavior in eq 3.19 as well as have a KIE magnitude that is normally

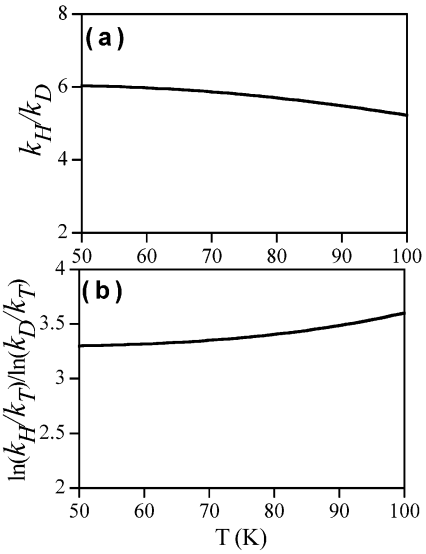

Figure 10. (a) k_H/k_D vs T eqs 2.17 and 2.18 with $\hbar\omega_Q = 435$ cm^{-1}, $V^{\ddagger} = 9.25$ kcal/mol, $E_S = 8$ kcal/mol, $\Delta Q = 0$, $m_Q = 20$ amu, $\hbar\omega_H = 3200$ cm^{-1}, $\hbar\omega_H^{\ddagger} = 2700$ cm^{-1}, and $\alpha_H = 32.3$ Å^{-1}. D and T parameters are appropriately mass scaled. (b) Swain−Schaad ratio $\ln(k_H/k_T)/\ln(k_D/k_T)$ vs T for system in part a.

consistent with adiabatic nontunneling PT, i.e., $k_H/k_D \leq 6$ at $T = 300$ K.[1,13,14,30]

3c.1. Low Temperature. We begin this analysis with the low T limit $\beta\hbar\omega_Q \gg 1$, where the KIE can be written as (cf. eqs 2.6 and 3.10)

$$k_{L1}/k_{L2} = C_{oL1}{}^2(Q_{eq})/C_{oL2}{}^2(Q_{eq}) \times \exp\left[(\alpha_{L1} - \alpha_{L2})\Delta Q + \frac{E_{\alpha L1} - E_{\alpha L2}}{\hbar\omega_Q}\right]$$

$$= \sqrt{\frac{m_{L2}}{m_{L1}}} \exp\left[-\frac{2\pi V^{\ddagger}}{\hbar\omega_H^{\ddagger}}(\sqrt{m_{L1}} - \sqrt{m_{L2}})\right] \times \exp\left[(\sqrt{m_{L1}} - \sqrt{m_{L2}})\alpha_H\Delta Q + \frac{E_{\alpha H}(m_{L1} - m_{L2})}{\hbar\omega_Q}\right] \quad (3.20)$$

The last line was obtained with eq 2.3 and the mass scaling $\alpha_L \propto \sqrt{m_L}$ and $\omega_L \propto \sqrt{1/m_L}$. With eq 3.20, one can ask the following question: With what system can one find eq 3.19 and a minimal KIE magnitude, and still remain in this regime $\beta\hbar\omega_Q \gg 1$? Figure 10 displays the KIE (H vs D) and Swain−Schaad ratio for a PT system with $\Delta G_{RXN} = 0$, $\Delta Q = 0$, $V^{\ddagger} = 9.25$ kcal/mol, $\alpha_H = 32.3$ Å^{-1} (α_D and α_T mass scaled) and $\hbar\omega_Q = 435$ cm^{-1}. Remarkably, the KIE magnitude and Swain−Schaad ratio are what one might associate with *nontunneling* PT. However, this occurs at *extremely* low temperatures (50−100 K), where even for *nontunneling* PT, the KIE is expected to be much larger. Only at these temperatures is it possible to numerically obtain the characteristic KIE ratios and a minimal KIE, while simultaneously keeping $\beta\hbar\omega_Q \gg 1$.[49] We now consider higher and more experimentally reasonable temperatures.

3c.2. Moderate to High Temperatures. For this tunneling regime, we return to Figure 6. For the magnitude of the H vs D KIE, there is already certainly consistent with nontunneling, but is the Swain−Schaad relationship satisfied? Figure 11 displays the deuterium vs tritium KIE for the Figure 6 case, and one notices immediately that the KIE is predominantly inverse,

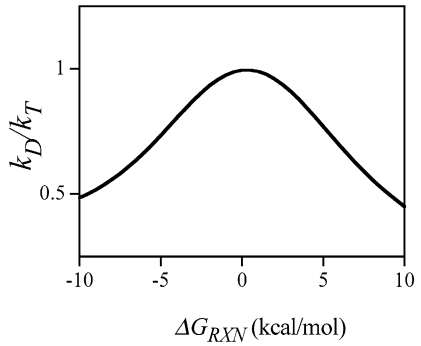

Figure 11. k_D/k_T for PT system in Figure 7 ($\hbar\omega_Q = 300$ cm^{-1}).

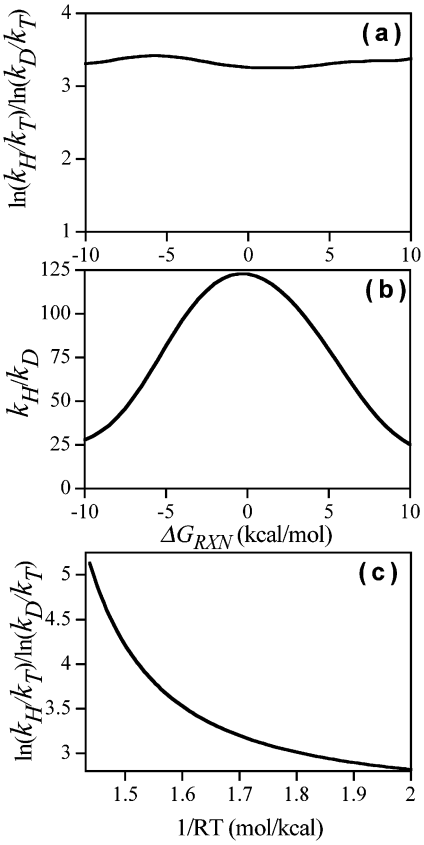

Figure 12. (a) Swain−Schaad ratio $\ln(k_H/k_T)/\ln(k_D/k_T)$ vs reaction asymmetry for same PT system as in Figure 7 ($T = 300$ K), except $\hbar\omega_Q = 375$ cm^{-1}. (b) k_H/k_D for system in part a. (c) $\ln(k_H/k_T)/\ln(k_D/k_T)$ vs $1/RT$ ($T = 250$−350 K) for symmetric reaction in part a.

except near $\Delta G_{RXN} = 0$, where it is unity. The source of this KIE inversion is the same as described in section 3a in connection with KIE vs reaction asymmetry: heavier particles preferentially benefit from excitation of both the H-bond and L mode, especially for more asymmetric reactions. In this particular case, these excitations make Triton transfer more facile than D transfer. The Swain−Schaad ratio in this case would be ridiculous to compute, because it is negative. This system, however, illustrates a possible KIE regime: a low-frequency H-bond mode that produces a small H vs D KIE could also produce an inverse D vs T KIE $k_T \geq k_D$.

We now consider systems where a positive Swain−Schaad ratio can be obtained in the moderate to high T limit. Figure 12a displays that ratio for the same system in Figure 11 except the H-mode frequency has been increased to $\hbar\omega_Q = 375$ cm^{-1} ($T = 300$ K). The Swain−Schaad ratio is at the expected value eq 3.19, but the H vs D KIE (displayed in Figure 12b) is clearly large enough to indicate tunneling PT. Furthermore, the T-

variation of the Swain−Schaad ratio for this system, displayed in Figure 12c, shows a distinct deviation from eq 3.19 for part of the temperature range, and thus also allows confirmation of tunneling PT.[50] This example clearly illustrates the advantage of varying systems parameters such as T and reaction asymmetry to identify tunneling with specific KIE aspects.

4. Concluding Remarks

A theoretical description of primary kinetic isotope effects (KIEs) has been presented for proton-transfer reactions, of the acid−base variety within a hydrogen-bonded complex, in the tunneling regime. This treatment differs from traditional descriptions of tunneling PT in that external environmental rearrangement is the reaction coordinate. Four individual KIE aspects—including KIE magnitude, temperature dependence, variation with reaction asymmetry, and adherence to the Swain−Schaad relationship—have been analyzed for tunneling PT reactions. It has been shown that a number of the predictions for these trends are quite similar to those expected from traditional treatments that do *not* include tunneling. In general, the clear identification of tunneling behavior is not straightforward for PT reactions involving strong coupling to the environment. Deviation from Swain−Schaad behavior is the most likely indicator of tunneling PT[2] (cf. section 3c), but generally it is the *combination* of these four KIE behaviors, with special emphasis on variation with reaction asymmetry or temperature, which clearly allows for identification of tunneling PT systems.

An additional criteria exists for identifying a PT system as being in the tunneling regime, namely the existence of an "inverted" regime.[43] An "inverted" regime has been experimentally observed for some PT systems,[44] but clarification is required concerning the conditions necessary for its existence, especially considering the contribution of excited-state reaction asymmetry dependencies to the total rate, as displayed in Figure 6.[43] These issues are the subject of future work.

The sensitivity to excitation of the H-bond and proton vibrational modes is a key factor that determines the behavior of several KIE features. Notably, these modes are more accessible for asymmetric reactions, and because excitation in these modes increases the tunneling probability,[39] asymmetric reactions can be dominated by these excitations. The fact that, compared to the proton, the deuteron is more sensitive to the H-bond dynamics and is easier to excite implies that H-bond and deuteron excitation increase the D transfer rate more than is the case for H. The result is a k_H/k_D KIE that decreases with increased reaction asymmetry as well as with temperature.

A prescription for interpreting slopes in an Arrhenius plot for tunneling rate constants and KIEs is a key result of this work, i.e., eq 3.14. Thermal excitations of the proton/deuteron and H-bond modes explicitly contribute to the effective activation energy, in addition to the actual reaction free energy barrier, and in some cases, these excitations can dominate the effective activation energy.

We now briefly comment on the critical parameters involved in the application of the nonadiabatic PT formalism, including further aspects to consider besides the simple model presented here.[51] These include the proton barrier $V^{\ddagger}$ at the H bond equilibrium position Q_{eq}, the solvent reorganization energy E_S, and the H-bond mode frequency ω_Q. We focus on these since other parameters, including the frequencies for the proton well $\omega_{R,P}$ and barrier $\omega^{\ddagger}$, the exponential coupling coefficient α_H—and their deuterated counterparts, and the effective mass of the H-bond coordinate m_Q can be estimated based on the system characteristics.[3b,5e] Since $V^{\ddagger}$ depends on Q_{eq}, the H-bond mode remains a key component, with both its frequency and equilibrium separation to be determined. The solvent reorganization energy E_S defines the last undetermined parameter. Two of the three parameters that would be "fit" to experimental data, ω_Q and E_S, are also critical to the effective activation energy E_{AL}. These uncertainties require that care be taken when interpreting the H-bond characteristics and solvent reorganization energy. In particular, the unknown H-bond separation and frequency may not be uniquely defined; for example, a decrease in KIE may be due to either a decreased H-bond separation or a decreased H-bond frequency. These difficulties would be reduced by insisting that the fit parameters apply to several rate constant and KIE features simultaneously.

The developments and calculations in this paper have employed several simplifications, specifically, the neglect of any temperature dependence of the environmental polarity (which can give, e.g., a temperature-dependent reorganization), as well as of other H-bond properties often present in real systems, anharmonicity and "intrinsic" asymmetry. While the general picture for KIE behaviors presented is not significantly altered by ignoring these effects, they may need to be taken into account in a detailed analysis of individual systems.

Concerning the first simplification, solvent polarity is known to significantly change with temperature, and this change translates into a decrease in reorganization energy with increasing T,[34,47] decreasing the effective activation energy. Of course, the reorganization energy is not determined solely by polarity, but often it is best described by environmental rearrangement including nuclear rearrangement of bonding surrounding the H-bond complex.[19] For complex environments, like proteins, simulation will provide the best source for evaluation and interpretation of reorganization energies (e.g., see ref 6). As for the remaining simplifications, weak H-bond complexes have properties that deviate from the simple harmonic oscillator model used here, including anharmonicity and asymmetry between the reactant and product.[37] Anharmonicity in Q will decrease the thermal accessibility of smaller Q separations that promote tunneling, and thus also lead to decreased effective activation energies.[5,34] The asymmetry in Q, i.e., ΔQ (cf. ΔQ and E_Q in eq 2.11) also affects the proton coupling C and thus will contribute to the Q motion averaging component in E_{AL}.

Acknowledgment. This work was supported in part by NSF Grants CHE-9700419, CHE-0108314, and CHE-0417570 and the Cristol Fund from the Department of Chemistry and Biochemistry at the University of Colorado at Boulder. P.M.K. acknowledges the support of an NIH Postdoctoral Fellowship (4/98-3/00).

Appendix A. Free Energy Relationship (FER) for Nonadiabatic Proton Transfer

In this Appendix, an isotope-dependent FER of the form of eq 3.1 is derived for the moderate to high-temperature regime. We begin the analysis with the PT rate expression in this regime, cf. eqs 2.17 and 2.24

$$k_L = \sum_{n_R}\sum_{n_P} P_{n_R} \frac{\langle C_{n_R,n_P}{}^2 \rangle}{\hbar} \sqrt{\frac{\pi}{(E_S + \tilde{E}_{\alpha L})RT}} \exp\left[-\frac{\Delta G^{\ddagger}_{n_R,n_P}}{RT}\right] \tag{A.1}$$

and rewrite it in terms of the rate constant involving only the 0−0 proton transition and the remaining contribution from

excited states. For this purpose, the thermal average over the squared proton coupling in eq 2.23 can be re-expressed in terms of that for the 0−0 case (see eq 2.21)

$$\langle C_{n_R,n_p}{}^2\rangle = \langle C_{0,0}{}^2\rangle \exp\left[\frac{\pi(\hbar\omega_R n_R + \hbar\omega_P n_P)}{\hbar\omega^{\ddagger}}\right] \quad \text{(A.2)}$$

and the 0−0 free energy barrier $\Delta G^{\ddagger}_{Lo,o}$ can also be isolated within the general activation free energy in eq 2.25,

$$\Delta G^{\ddagger}_{n_R,n_p} = \Delta G^{\ddagger}_{L0,0} + \Delta\Delta G^{\ddagger}_{n_R,n_p} \quad \text{(A.3)}$$

where

$$\Delta G^{\ddagger}_{L0,0} = \frac{(\Delta G_{RXN} + E_S + E_{\alpha L})^2}{4(E_S + \tilde{E}_{\alpha L})} \quad \text{(A.4)}$$

$$\Delta\Delta G^{\ddagger}_{n_R,n_p} = [(n_P\hbar\omega_P - n_R\hbar\omega_R)(2(\Delta G_{RXN} + E_S + E_{\alpha L}) + n_P\hbar\omega_P - n_R\hbar\omega_R)]/4(E_S + \tilde{E}_{\alpha L}) \quad \text{(A.5)}$$

The rate expression in eq A.1 can now be written as

$$k_L = k_{L00}\sum_{n_R,n_P} F_{n_R,n_P} = k_{L00}\rho_L \quad \text{(A.6)}$$

in terms of the 0−0 rate constant

$$k_{L00} = \frac{\langle C_{0,0}{}^2\rangle}{\hbar}\sqrt{\frac{\pi}{(E_S + \tilde{E}_{\alpha L})RT}}\exp\left[-\frac{\Delta G^{\ddagger}_{L0,0}}{RT}\right] \quad \text{(A.7)}$$

where the coefficient of each transition F_{n_R,n_P} is

$$F_{n_R,n_P} = P_{n_R}\exp\left[\frac{\pi(\hbar\omega_R n_R + \hbar\omega_P n_P)}{\hbar\omega^{\ddagger}}\right]\exp\left[-\frac{\Delta\Delta G^{\ddagger}_{n_R,n_P}}{RT}\right] \quad \text{(A.8)}$$

The second expression in eq A.6 denotes the sum as an enhancement factor ρ_L of the rate due to excited proton states. With the hindsight that the KIE vs ΔG_{RXN} behavior is maximal near $\Delta G_{RXN} = 0$, we focus our attention of this behavior near $\Delta G_{RXN} = 0$. We start with the natural logarithm of eq A.6

$$\ln k_L = \ln k_{L00} + \ln\left[\sum_{n_R,n_P} F_{n_R,n_P}\right] \quad \text{(A.9)}$$

From eq A.7, the first term in eq A.9 is

$$\ln k_{L00} = \ln\left[\frac{\langle C_{0,0}{}^2\rangle}{\hbar}\sqrt{\frac{\pi}{(E_S + \tilde{E}_{\alpha L})RT}}\right] - \frac{\Delta G^{\ddagger}_{0,0}}{RT} \quad \text{(A.10)}$$

which is second order in ΔG_{RXN} via eq A.4. The second term in eq A.9 is now expanded up to second order in ΔG_{RXN}, near $\Delta G_{RXN} = 0$

$$\ln\left[\sum_{n_R,n_P} F_{n_R,n_R}\right] = \ln\left[\sum_{n_R,n_P} F_{n_R,n_R}|_o\right] + \frac{\Delta G_{RXN}}{\sum_{n_R,n_P} F_{n_R,n_P}|_o}\sum_{n_R,n_P}\left.\frac{\partial F_{n_R,n_P}}{\partial\Delta G_{RXN}}\right|_o + \frac{\Delta G_{RXN}{}^2}{2}\frac{1}{\left(\sum_{n_R,n_P} F_{n_R,n_P}|_o\right)^2}\times \left[\left(\sum_{n_R,n_P} F_{n_R,n_P}|_o\right)\sum_{n_R,n_P}\left.\frac{\partial^2 F_{n_R,n_P}}{\partial\Delta G_{RXN}{}^2}\right|_o - \left(\sum_{n_R,n_P}\left.\frac{\partial F_{n_R,n_P}}{\partial\Delta G_{RXN}}\right|_o\right)^2\right] \quad \text{(A.11)}$$

F_{n_R,n_P} and its derivative are evaluated for $\Delta G_{RXN} = 0$

$$F_{n_R,n_P}|_o = \exp\left[\frac{\pi(\hbar\omega_R n_R + \hbar\omega_P n_P)}{\hbar\omega^{\ddagger}}\right]\exp\left[-\frac{\hbar\omega_R n_R + \Delta\Delta G^{\ddagger}_o}{RT}\right]$$

$$\left.\frac{\partial F_{n_R,n_P}}{\partial\Delta G_{RXN}}\right|_o = -\frac{1}{RT}\frac{\partial\Delta\Delta G^{\ddagger}_{n_R,n_P}}{\partial\Delta G_{RXN}}F_{n_R,n_P}|_o;$$

$$\left.\frac{\partial^2 F_{n_R,n_P}}{\partial\Delta G_{RXN}{}^2}\right|_o = \frac{1}{(RT)^2}\left(\frac{\partial\Delta\Delta G^{\ddagger}_{n_R,n_P}}{\partial\Delta G_{RXN}}\right)^2 F_{n_R,n_P}|_o \quad \text{(A.12)}$$

where $\Delta\Delta G^{\ddagger}_o$ is the reaction free energy contribution due to excited states $\Delta\Delta G^{\ddagger}_{n_R,n_P}$ (see eq 3.5) evaluated at $\Delta G_{RXN} = 0$

$$\Delta\Delta G_o{}^{\ddagger} = \{[n_P\hbar\omega_P - n_R\hbar\omega_R][2(E_S + E_{\alpha L}) + n_P\hbar\omega_P - n_R\hbar\omega_R]\}/4(E_S + \tilde{E}_{\alpha L}), \text{ and } \frac{\partial\Delta\Delta G^{\ddagger}_{n_R,n_P}}{\partial\Delta G_{RXN}} = \frac{n_P\hbar\omega_P - n_R\hbar\omega_R}{2(E_S + \tilde{E}_{\alpha L})} \quad \text{(A.13)}$$

With these results, eq A.11 is now

$$\ln\left[\sum_{n_R,n_P} F_{n_R,n_P}\right] = \ln\left[\sum_{n_R,n_P} F_{n_R,n_P}|_o\right] - \frac{\Delta G_{RXN}}{RT}\left\langle\frac{\partial\Delta\Delta G^{\ddagger}_{n_R,n_P}}{\partial\Delta G_{RXN}}\right\rangle_F + \frac{\Delta G_{RXN}{}^2}{2(RT)^2}\times \left[\left\langle\left(\frac{\partial\Delta\Delta G^{\ddagger}_{n_R,n_P}}{\partial\Delta G_{RXN}}\right)^2\right\rangle_F - \left\langle\frac{\partial\Delta\Delta G^{\ddagger}_{n_R,n_P}}{\partial\Delta G_{RXN}}\right\rangle_F{}^2\right] \quad \text{(A.14)}$$

where the average is over the probability distribution defined by $F_{n_R,n_P}|_o$, e.g.

$$\left\langle\frac{\partial\Delta\Delta G^{\ddagger}_{n_R,n_P}}{\partial\Delta G_{RXN}}\right\rangle_F = \frac{1}{\sum_{n_R,n_P} F_{n_R,n_P}|_o}\sum_{n_R,n_P} F_{n_R,n_P}|_o\frac{\partial\Delta\Delta G^{\ddagger}_{n_R,n_P}}{\partial\Delta G_{RXN}} \quad \text{(A.15)}$$

The coefficients in eq 3.1 are thus found to be eqs 3.6−3.8 of the text.

Appendix B. Arrhenius Behavior for Nonadiabatic Proton Transfer Kinetic Isotope Effects

In this Appendix, Arrhenius expressions for individual isotope rate constants as well as the KIE for a limited temperature range are derived. For this purpose, we consider the rate expression

eq A.1 referenced to the 0−0 rate constant, focusing first on putting the 0−0 PT rate constant (see eq A.7)

$$k_{L00} = \frac{\langle C_{0,0}{}^2 \rangle}{\hbar} \sqrt{\frac{\pi}{(E_S + \tilde{E}_{\alpha L})RT}} \exp\left[- \frac{\Delta G^{\ddagger}_{L0,0}}{RT} \right] \quad \text{(B.1)}$$

into an Arrhenius form, and we then describe the influence of excited proton states.

Here we expand the above rate expression around a given temperature in the middle of an experimental temperature range ($1/RT_o = \beta_o$):

$$\beta = \beta_o + \beta - \beta_o = \beta_o + \Delta\beta; \quad \varsigma = ({}^1/_2)\beta\hbar\omega_Q = \varsigma_o + \Delta\varsigma \quad \text{(B.2)}$$

with $\Delta\beta/\beta_o$ and $\Delta\zeta$ assumed to be small, $\ll 1$. For a small temperature range (300−350 K) this assumption works fairly well because the $\Delta\beta$ range is ~10%, while $\Delta\zeta \ll 1$ is valid as long as the Q mode does not have a very high frequency, $\omega_Q \leq 600\ \text{cm}^{-1}$. In this limit, keeping only linear terms in $\Delta\beta$, the hyperbolic cotangent is

$$\coth(\zeta) \approx \coth(\zeta_o) - ({}^1/_2)\Delta\beta\hbar\omega_Q[\coth^2(\zeta_o) - 1] \quad \text{(B.3)}$$

Equation 2.23 for 0−0 then becomes

$$\langle C_{0,0}{}^2 \rangle \approx C_{eqL0,0}{}^2 \exp\left(2 \coth(\zeta_o) \frac{E_{\alpha L}}{\hbar\omega_Q} \right) \times \exp(-\Delta\beta E_{\alpha L}[\coth^2(\zeta_o) - 1]) \quad \text{(B.4)}$$

Equation B.1 can now be written in an Arrhenius-like form ($k_L = A_L \exp(-\beta E_{AL})$):

$$k_{L00} = k_{oL} \exp(\beta_o E_{AL00}) \exp(-\beta E_{AL00}) \quad \text{(B.5)}$$

where the Arrhenius parameters have the following definitions

$$\ln A_L = \ln k_{oL} + \beta_o E_{AL}, \quad \text{and}$$
$$E_{AL00} = E_{\alpha L}[\coth^2(\zeta_o) - 1] + \Delta G^{\ddagger}_{L0,0} \quad \text{(B.6)}$$

$k_{oL} = k_{L00}(T_o)$ is just the 0−0 rate at the midrange temperature T_o, and

$$A_L = k_{oL} \exp(\beta_o E_{AL}) = \frac{C_{eqL}{}^2(Q_{eq})}{\hbar} \sqrt{\frac{\pi}{(E_S + \tilde{E}_{\alpha L})RT}} \times \exp\left(2\frac{E_{\alpha L}}{\hbar\omega_Q} \coth(({}^1/_2)\beta_o\hbar\omega_Q) + \beta_o E_{\alpha L}[\coth^2(\varsigma_o) - 1] \right) \quad \text{(B.7)}$$

We now consider excited proton vibrational states in a manner similar to that of Appendix A. Equation 3.3 is rewritten as

$$k_L = k_{oL} \exp(-\Delta\beta E_{AL00}) \sum_{n_R}\sum_{n_P} F_{oR,P} \times \exp[-\Delta\beta(\hbar\omega_R n_R + \Delta\Delta G^{\ddagger}_{n_R,n_P})] \quad \text{(B.8)}$$

where $F_{oR,P} = F_{n_R,n_P}(T = T_o)$ (see eq A.12). The slope of the natural logarithm of eq B.8 with respect to $\Delta\beta$ gives the activation energy E_{AL}

$$\ln(k_L) = \ln(k_{oL}) - \Delta\beta E_{AL00} + \ln\left\{ \sum_{n_R}\sum_{n_P} F_{oR,P} \exp[-\Delta\beta(\hbar\omega_R n_R + \Delta\Delta G^{\ddagger}_{n_R,n_P})] \right\} \quad \text{(B.9)}$$

To put eq B.9 into an Arrhenius form, a Taylor series expansion of its last term around $\Delta\beta = 0$ is performed

$$\ln\left\{ \sum_{n_R}\sum_{n_P} F_{oR,P} \exp[-\Delta\beta(\hbar\omega_R n_R + \Delta\Delta G^{\ddagger}_{n_R,n_P})] \right\} = \ln\left\{ \sum_{n_R}\sum_{n_P} F_{oR,P} \right\} - \Delta\beta \frac{\sum_{n_R}\sum_{n_P} F_{oR,P}(\hbar\omega_R n_R + \Delta\Delta G^{\ddagger}_{n_R,n_P})}{\sum_{n_R}\sum_{n_P} F_{oR,P}} - \ldots \quad \text{(B.10)}$$

Keeping only the leading orderterm in $\Delta\beta$, the linear term in $\Delta\beta$ is the weighted average of the additional activation by excited states

$$\langle \Delta\Delta G^{\ddagger}_{n_R,n_P} \rangle_L = \frac{\sum_{n_R}\sum_{n_P} F_{oR,P}(\hbar\omega_R n_R + \Delta\Delta G^{\ddagger}_{n_R,n_P})}{\sum_{n_R}\sum_{n_P} F_{oR,P}} \quad \text{(B.11)}$$

Equation B.11 is now in the desired Arrhenius form

$$\ln k_L = \ln k_{oL} + \ln\left\{ \sum_{n_R}\sum_{n_P} F_{oR,P} \right\} - \Delta\beta[E_{AL00} + \langle \Delta\Delta G^{\ddagger}_{n_R,n_P} \rangle_L] \quad \text{(B.12)}$$

with an Arrhenius activation energy given by

$$E_{AL} = E_{\alpha L}[\coth^2(\varsigma_o) - 1] + \Delta G^{\ddagger}_{L0,0} + \langle \Delta\Delta G^{\ddagger}_{n_R,n_P} \rangle_L \quad \text{(B.13)}$$

The middle term in eq B.12 is just $\ln \rho_L(T = T_o)$. The KIE at the reference temperature T_o is

$$\frac{k_H}{k_D} = \frac{k_{Ho}\rho_H(T_o)}{k_{Do}\rho_D(T_o)} = \frac{C_{eqH}{}^2\rho_H(T_o)}{C_{eqD}{}^2\rho_D(T_o)} \sqrt{\frac{E_S + \tilde{E}_{\alpha D}}{E_S + \tilde{E}_{\alpha H}}} \times \exp\left(-2\frac{E_{\alpha L}}{\hbar\omega_Q} \coth(({}^1/_2)\beta_o\hbar\omega_Q) \right) \exp\left[- \frac{\Delta G^{\ddagger}_{H0,0} - \Delta G^{\ddagger}_{D0,0}}{RT_o} \right] \quad \text{(B.14)}$$

The isotopic difference of the activation energies in eq B.13, e.g., H vs D, is

$$E_{AD} - E_{AH} = E_{\alpha H}[\coth^2(\varsigma_o) - 1] + \Delta G^{\ddagger}_{D0,0} - \Delta G^{\ddagger}_{H0,0} + \langle \Delta\Delta G^{\ddagger}_{n_R,n_P} \rangle_D - \langle \Delta\Delta G_{n_R,n_P}{}^{\ddagger} \rangle_H \quad \text{(B.15)}$$

References and Notes

(1) (a) Bell, R. P. *The Proton in Chemistry*, 2nd ed.; Cornell University Press: Ithaca, NY, 1973. (b) Caldin, E.; Gold, V. *Proton-Transfer Reactions*; Chapman and Hall: London, 1975. (c) Kresge, A. J. *Acc. Chem. Res.* **1975**, *8*, 354. (d) Hibbert, F. *Adv. Phys. Org. Chem.* **1986**, *22*, 113. Hibbert, F. *Adv. Phys. Org. Chem.* **1990**, *26*, 255.

(2) (a) Cha, Y.; Murray, C. J.; Klinman, J. P. *Science* **1989**, *243*, 1325.-(b) Kohen, A.; Klinman, J. P. *Acc. Chem. Res.* **1998**, *31*, 397. (c) Kohen, A.; Klinman, J. P. *Chem. Biol.* **1999**, *6*, R191. (d) Kohen, A.; Cannio, R.; Bartolucci, S.; Klinman, J. P. *Nature (London)* **1999**, *399*, 496.

(3) (a) Rickart, K. W.; Klinman, J. P. *Biochemistry* **1999**, *38*, 12218. (b) Knapp, M. J.; Rickart, K. W.; Klinman, J. P. *J. Am. Chem. Soc.* **2002**, *124*, 3865.

(4) (a) Basran, J.; Sutcliffe, M. J.; Scrutton, N. S. *Biochemistry*, **1999**, *38*, 3218. (b) Harris, R. J.; Meskys, R.; Sutcliffe, M. J.; Scrutton, N. S. *Biochemistry*, **2000**, *39*, 1189. (c) Basran, J.; Patel, S.; Sutcliffe, M. J.; Scrutton, N. S. *J. Biol. Chem.* **2001**, *38*, 3218.

(5) (a) Borgis, D.; Hynes, J. T. *J. Phys. Chem.* **1996**, *100*, 1118. (b) Borgis, D.; Hynes, J. T. *Chem. Phys.* **1993**, *170*, 315. (c) Borgis, D.; Lee, S.; Hynes, J. T. *Chem. Phys. Lett.* **1989**, *162*, 19. (d) Borgis, D.; Hynes, J. T. *J. Chem. Phys.* **1991**, *94*, 3619. (e) Lee, S.; Hynes, J. T. *J. Chim. Phys.* **1996**, *93*, 1783.

(6) (a) Agarwal, P. K.; Billeter, S. R.; Hammes-Schiffer, S. *J. Phys. Chem. B* **2002**, *106*, 3283. (b) Agarwal, P. K.; Billeter, S. R.; Rajagopalan, P. T.; Benkovic, S. J.; Hammes-Schiffer, *Proc. Natl. Acad. Sci. U.S.A.* **2002**, *99*, 2794. (c) Hammes-Schiffer, S. *Chem. Phys. Chem.* **2002**, *3*, 33. (d) Hammes-Schiffer, S.; Billeter, S. R. *Int. Rev. Phys. Chem.* **2001**, *20*, 591. (e) Billeter, S. R.; Webb, S. P.; Agarwal, P. K.; Iordanov, T.; Hammes-Schiffer, S. *J. Am. Chem. Soc.* **2001**, *123*, 11262. (f) Billeter, S. R.; Webb, S. P.; Iordanov, T.; Agarwal, P. K.; Hammes-Schiffer, S. *J. Chem. Phys.* **2001**, *114*, 6925. (g) Hammes-Schiffer, S. *Curr. Opin. Struct. Biol.* **2004**, *14*, 192.

(7) (a) Basner, J. E.; Schwartz, S. D. *J. Phys. Chem. B* **2004**, *108*, 444. (b) Antoniou, D.; Schwartz, S. D. *Proc. Natl. Acad. Sci. U.S.A.* **1997**, *94*, 12360. (c) Antoniou, D.; Schwartz, S. D. *J. Chem. Phys.* **1999**, *110*, 465. (d) Karmacharya, R.; Schwartz, S. D. *J. Chem. Phys.* **1999**, *110*, 7376.

(8) We refer to proton transfer throughout, but the theory applies to H atom and hydride transfer as well with special considerations. For the solvent coordinate picture presented here, the nonadiabatic PT formalism assumes that the electronic adiabatic proton potentials can be described by two electronic VB states, one for reactant and one for product. This picture has previously been applied to H atom transfer,[5e] but for some H atom or hydride transfer reactions more than two VB states may be required. In particular, proton coupled-electron-transfer reactions in which electron transfer over a large distance is coupled with proton transfer is thought to require multiple solvent coordinates, in addition to several VB states.[9, 10.]

(9) (a) Cukier, R. I. *J. Phys. Chem.* **1996**, *100*, 15428. (b) Cukier, R. I.; Nocera, D. *Annu. Rev. Phys. Chem.* **1998**, *49*, 337.

(10) (a) Soudackov, A.; Hammes-Schiffer, S. *J. Chem. Phys.* **2000** *113*, 2385. (b) Iordanova, N.; Decornez, H.; Hammes-Schiffer, S. *J. Am. Chem. Soc.* **2001**, *123*, 3723. (c) Iordanova, N.; Hammes-Schiffer, S. *J. Am. Chem. Soc.* **2002**, *124*, 4848. (d) Hammes-Schiffer, S. *Acc. Chem. Res.* **2001**, *34*, 273.

(11) Swain, G. G.; Stivers, E. C.; Reuwer, J. F.; Schaad, L. J. *J. Am. Chem. Soc.* **1958**, *80*, 5885.

(12) (a) Cukier, R. I. *J. Phys. Chem. B*, **2002**, *106*, 1746. (b) Cukier, R. I.; Zhu, J. *J. Phys. Chem. B* **1997**, *101*, 7180.

(13) (a) Westheimer, F. H. *Chem. Rev.* **1961**, *61*, 265. (b) Melander, L. *Isotope Effects on Reaction Rates*; The Ronald Press Co.: New York, 1960.

(14) Melander, L.; Saunders, W. H. *Reaction Rates of Isotopic Molecules*; Wiley: New York, 1980.

(15) For tunneling calculations consistent with the stanadard view, see: (a) Alhambra, C.; Corchado, J. C.; Sánchez, M. L.; Gao, J.; Truhlar, D. G. *J. Am. Chem. Soc.* **2000**, *122*, 8197. (b) Hwang, J.-K.; Warshel, A.*J. Phys. Chem.* **1993,** *97*, 10053. (c) Hwang, J.-K.; Chu, Z. T.; Yadav, A.; Warshel, A.*J. Phys. Chem.* **1991,** *95*, 8445. (d) Hwang, J.-K.; Warshel, A. *J. Am. Chem. Soc.* **1996**, *118*, 11745. (e) Alhambra, C.; Gao, J.; Corchado, J. C.; Villa, J.; Truhlar, D. G. *J. Am. Chem. Soc.* **1999**, *121*, 2253. (f) Cui, Q.; Karplus, M. J. Am. Chem. Soc. **2002**, *124*, 3093.

(16) (a) Bell, R. P. *The Tunnel Effect in Chemistry*; Chapman and Hall: NewYork, 1980. (b) Bell, R. P.; Sachs, W. H.; Tranter, R. L. *Trans. Far. Soc.* **1971**, *67*, 1995.

(17) (a) Babamov, V. K.; Marcus, R. A. *J. Chem. Phys.* **1981**, *74*, 1790. (b) Hiller, C.; Manz, J.; Miller, W. H.; Römelt, J. *J. Chem. Phys.* **1983**, *74*, 3850. (c) Miller, W. H. *J. Am. Chem. Soc.* **1979**, *101*, 6819. (d) Skodje, R. T.; Truhlar, D. G.; Garrett, B. C. *J. Chem. Phys.* **1982**, *77*, 5955. (e) Marcus, R. A.; Coltrin, M. E. *J. Chem. Phys.* **1977.** *67*, 2609. (f) Garrett, B. C.; Truhlar, D. G. *J. Chem. Phys.* **1983**, *79*, 4931. (g) Kim, Y.; Kreevoy, M. M. *J. Am. Chem. Soc.* **1992**, *114*, 7116.

(18) (a) Dogonadze, R. R.; Kuznetzov, A. M.; Levich, V. G. *Electrochim. Acta* **1968**, *13*, 1025. (b) German, E. D.; Kuznetzov, A. M.; Dogonadze, R. R. *J. Chem. Soc., Faraday Trans. 2* **1980**, *76*, 1128. (c) Kuznetzov, A. M. *Charge Transfer in Physics, Chemistry and Biology: Physical Mechanisms of Elementary Processes and an Introduction to the Theory*; Gordon and Breach Publishers: Amsterdam, 1995. (d) Kuznetzov, A. M.; Ulstrup, J. *Can. J. Chem.* **1999**, *77*, 1085. (e) Sühnel, J.; Gustav, K. *Chem. Phys.* **1984**, *87*, 179.

(19) (a) Ando, K.; Hynes, J. T. *J. Phys. Chem. B* **1997**, *101*, 10464. (b) Ando, K.; Hynes, J. T. *J. Phys. Chem. A* **1999**, *103*, 10398. (c) Staib, A.; Borgis, D.; Hynes, J. T. *J. Chem. Phys.* **1995**, *102*, 2487. (d) Ando, K.; Hynes, J. T, *Adv. Chem. Phys.*, **1999**,*110*, 381.

(20) (a) Basilevsky, M. V.; Soudackov, A.; Vener, M. V. *Chem. Phys.* **1995**, *200*, 87. (b) Basilevsky, M. V.; Vener, M. V.; Davidovich, G. V.; Soudackov, A. *Chem. Phys.* **1996**, *208*, 267. (c) Vener, M. V.; Rostov, I. V.; Soudackov, A.; Basilevsky, M. V. *Chem. Phys.* **2000**, *254*, 249.

(21) (a) Kiefer, P. M.; Hynes, J. T. *J. Phys. Chem. A* **2002**,*106*, 1834. (b) Kiefer, P. M.; Hynes, J. T. *J. Phys. Chem. A* **2002**,*106*, 1850.

(22) The expression in eq 2.1 is similar in form to that for weakly electronically coupled (electronically nonadiabatic) electron transfer,[23] in that the proton coupling C is analogous to the electronic resonance coupling and the reorganization energy E_S is analogous to the electronic *diabatic* solvent reorganization energy. Even though the reorganization energies and couplings are analogous, the physical picture behind the two reaction types is quite different.[24] The reorganization energy for proton tunneling is the free energy difference associated with a Franck−Condon-like excitation (all nuclear and solvent modes other than the proton mode are held fixed) of the ground *diabatic* proton vibrational state at the equilibrium reactant solvent position to the ground product *diabatic* proton vibrational state, followed by relaxation along the solvent coordinate to the equilibrium solvent product position (see Figure 1d).

(23) (a) Marcus, R. A. *J. Chem. Phys.* **1956**, *24*, 966; 979. (b) Marcus, R. A.; Sutin, N. *Biochim. Biophys. Acta* **1985**, *811*, 265. (c) Sutin, N. *Prog. Inorg. Chem.* **1983**, *30*, 144.

(24) The electronic resonance coupling is qualitatively described by the overlap between two electronic *diabatic* states, while the proton coupling is described by the overlap between two *nuclear* diabatic proton wave functions. The reorganization energy for ET is defined from a electronically *diabatic* perspective, and is defined[23] by the free energy difference associated with a Franck−Condon electronic excitation from the equilibrium reactant solvent position on the reactant electronic diabatic surface to the product electronic *diabatic* state, followed by relaxation in a solvent coordinate to the equilibrium product position.

(25) As noted above, the terms adiabatic and nonadiabatic refer to the proton vibrational states. A Born−Oppenheimer approximation between the electronic and nuclear degrees of freedom is always assumed, with nuclear motion (including proton motion) occurring on an electronically *adiabatic* surface. For PT within a H-bonded complex, the electronic coupling between electronic diabatic states is significant, ∼1 eV.[5,19,21] This contrasts with weakly coupled electron transfer (ET), where the electronic coupling is much smaller.[23] In the latter special case of weakly coupled ET the transfer of a proton can accompany ET.[9,10]

(26) For example, the cutoff equilibrium H-bond separation between adiabatic and nonadiabatic PT is ∼2.7Å for OH···O systems.[27, 28.]

(27) Kiefer, P. M.; Leite, V. P. B.; Whitnell, R. M. *Chem. Phys.* **1995**, *194*, 33.

(28) (a) Novack, A. *Struct. Bonding (Berlin)* **1974**, *18*, 177. (b) Zeegers-Huyskens, T.; Huyskens, P. In *Molecular Interactions*; Ratajcak, H, Orville-Thomas, W. J., Eds.; John Wiley & Sons: New York, 1980; Vol. 2, p 1.

(29) Some PT systems will undoubtedly contain a mixture of nonadiabatic and adiabatic behavior. For example, the proton could be thermally excited where the proton vibrational state is above the barrier in the proton coordinate or it can tunnel through the proton barrier. The rate for the mixed case is the sum of the adiabatic and nonadiabatic PT rates, and the KIEs would thus be a convolution of adiabatic and nonadiabatic PT KIEs. See examples in ref 6.

(30) Kiefer, P. M.; Hynes, J. T. *J. Phys. Chem. A.* **2003**, *107*, 9022.

(31) (a) Child, M. S. *Molecular Collision Theory*; Academic Press: New York, 1974. (b) W. H. Miller, *J. Phys. Chem.* **1979**, *83*, 960−963. (c) Rapp, D. *Quantum Mechanics*; Holt, Rinehart, and Winston, Inc.: San Francisco, CA, 1971.

(32) Jaroszewski, L.; Lesyng, B.; Tanner, J. J.; McCammon, J. A. *Chem. Phys. Lett.* **1990**, *175*, 282.

(33) Nonlinear corrections to eq 2.4 exist, but only become significant when the Q motion is quite anharmonic and the range of vibrational motion expands beyond several tenths of an angstrom.[5d,18] Henceforth, we assume the linear exponential form in eq 2.4.

(34) Kiefer, P. M.; Hynes, J. T. *Isr. J. Chem.* **2004**, *44*, 171.

(35) Electronic resonance coupling for weakly coupled ET has the same exponential form as eq 2.4, with[23] $\alpha_{ET} \sim 1$ Å^{-1}, a value also consistent with the mass dependence.

(36) The in-plane bending mode is definitely coupled with the H-bond mode Q. In particular, a strongly bent H-bond system will have a larger effective Q_{eq} as well as a strong coupling between the bend mode and excited proton vibrational states.[30] Here we consider a linear H-bond system, where any bending contributions have been renormalized into the single H-bond mode frequency and separation. For simulation examples where the proton coordinate is treated with a stretch and bend, see ref 6.

(37) We note that anharmonic models have been used in the past but do not significantly alter the picture and resulting KIE trends.[5d, e.]

(38) As a final note on eq 2.13, its low-temperature limit is not eq 2.5; i.e., the average in eq 2.16 does not give eq 2.6 for low temperatures $RT \ll$

$\hbar\omega_Q$. Equation 2.5 and 2.13 are two limits of the general rate expression for proton tunneling including Q vibration given in eq 2.10.[5a]

(39) The H-bond vibrational mode is assumed in this paper to remain significantly unchanged while the reaction coordinate fluctuates from the 0−0 TS to either the 0−1 or 1−0 TS.

(40) Model calculations using a two VB model for an OH···O proton potential similar to that used in ref 21 give proton couplings consistent with those evaluated via eq 2.21, i.e., to within 20%. The $(1/2)(n_R\hbar\omega_R + n_P\hbar\omega_P)$ term in eq 2.21 is an estimate for the decrease in barrier height for excited states.

(41) The approximations that α_L is transition-independent and eq 2.21 for the transition dependence of C_{eqL} are based on model calculations by the present authors. Furthermore, these approximations are key provisions that allow for the development of the quantitative analysis in section 3, specifically those that indicate explicit contributions from excited proton states. While slight deviations from these approximations are possible and likely for real systems, the quantitative trends that result from the present analysis are not significantly altered by such deviations.

(42) In the standard picture including tunneling, KIEs are also expected to exhibit a maximum for $\Delta G_{RXN} = 0$[13, 14, 16]. For a one-dimensional barrier, the tunneling correction is determined by the imaginary frequency (determined by the force constant and mass of the TS mode). The Westheimer−Melander picture[13,14] for nontunneling PT states that for a symmetric reaction the TS mode is purely classical proton motion, so that the TS mode includes more of the donor−acceptor mode as the reaction becomes more a symmetric. Thus, the TS mode mass increases with reaction asymmetry, and tunneling by H (or D) is less with increasing asymmetry, giving a maximal KIE for pure H (or D) motion for symmetric reaction and lower KIEs for less H (or D) tunneling at TS.

(43) Note that the total rate constants for H and D transfer in Figure 6 increase with increased exothermicity. The significant contribution of excited proton states to the rate constant in the present model calculations precludes the possibility of any 'inverted' regime for tunneling PT; i.e., the rate constant continues to increase for increased reaction exothermicity. Conversely, suppression of these excited-state contributions would give an inverted region behavior. While experiments[44] demonstrate that an 'inverted' regime is possible for PT, the physical aspects of these systems that allow for observation of an 'inverted' regime remain to be clarified.

(44) (a) Peters, K. S.; Cashin, A.; Timbers, P. *J. Am. Chem. Soc.* **2000**, *122*, 107. (b) Peters, K. S.; Cashin, A. *J. Phys. Chem. A* **2000**, *104*, 4833. (c) Peters, K. S.; Kim, G. *J. Phys. Chem. A* **2001**, *105*, 4177. (c) Andrieux, C. P.; Gamby, J.; Hapiot, P.; Saveant, J.-M. *J. Am. Chem. Soc.* **2003**, *125*, 10119.

(45) For the present system, the numerical deviation from $^1/_2$ is ∼5%. However, using the full state-to-state rate constant eqs 2.17 with eq 2.18, instead of eq 2.17 with eq 2.24, the numerical deviation from $^1/_2$ is <0.1%. This denotes the sensitivity at which eq 2.24 will break down. Note that $\bar{\alpha}_{oL} \neq {}^1/_2$ is expected for an intrinsically asymmetric reaction (i.e., $\Delta Q \neq 0$, not considered within). Furthermore, the noticeable deviation from $\bar{\alpha}_{oL} \neq {}^1/_2$ for $\Delta Q \neq 0$ is isotope-dependent, and thus the maximum in a KIE vs reaction asymmetry plot will be shifted away from $\Delta G_{RXN} = 0$.

(46) Of course, in the solution case, the solvent would need to remain liquid and classical. More generally, the environment would have to remain classical.

(47) On the basis of the PT model used in refs 21 and 34, the reorganization energy E_S for nonadiabatic PT can be described with the following microscopic quantities: $E_S = (1/2)K(\mu_R - \mu_P)^2(\Delta c_P^2)^2$, where K contains the dependence on solvent polarity via the static and optical dielectric constants: $K = 2M_S(1/\epsilon_\infty - 1/\epsilon_o)$. M_S is a factor dependent on the structure of the H-bond complex. The remaining terms describe the difference in reactant and product electronic structures: μ_R and μ_P are the electronically diabatic dipole moments of the H-bond complex for the reactant and product, and Δc_P^2 is the difference, between the reactant and product, in the contributions of the product valence bond state to the electronic structure. The T dependence of E_S stems from the T dependence of the static dielectric constant ϵ. In model calculations for nontunneling PT[34] we have included the T dependence of the dielectric constant ϵ of water and find (i) a ∼20% reduction of the rate Arrhenius slopes and (ii) only a slight effect (<5%) on the KIE Arrhenius slope.

(48) This is particularly true for H atom transfer reactions because they are weakly coupled to a polar environment, i.e., small reorganization energies (cf. the H atom transfer reaction in ref 5e).

(49) Because this system has a low proton barrier $V^\ddagger = 9.25$ kcal/mol, the proton or deuteron could be excited to a vibrational state above the proton barrier, and PT would then proceed via a nontunneling process. At this low T, however, the rate constant for such a process is many order of magnitudes smaller (for both H and D) than the tunneling rate constants.

(50) In Figure 12c, the Swain−Schaad ratio increases from that expected by eq 3.19 with increased temperature. This T behavior is due to the relative decrease in KIE (k_H/k_T vs k_D/k_T) as T is increased. The relative decrease is due to the magnitude of each KIE and the difference in effective activation energies E_{AL}s that determines each KIEs' T dependence $\{(E_{AT} - E_{AH})\}/\{\ln(k_H/k_T)_{T_o}\} < \{(E_{AT} - E_{AD})\}/\{\ln(k_D/k_T)_{T_o}\}$. If a PT system was in the nontunneling regime at high temperatures one might expect that lowering the temperature would put the PT system in the tunneling regime, and thus one would expect a large Swain−Schaad ratio at low temperatures that progressively decreases toward the expected value eq 3.19 as T is increased. Figure 12c, however, displays the T dependence for a PT system that remains in the tunneling regime at all the displayed temperatures.

(51) This formalism has already been applied to an H atom transfer reaction,[5e] where the coupling to the solvent is weak, and e.g., the temperature dependence and KIE magnitude are quite different from those found in the present work.